



Cite this: DOI: 10.1039/c5ob01843a

Arginine analogues incorporating carboxylate bioisosteric functions are micromolar inhibitors of human recombinant DDAH-1†

Sara Tommasi,^{a,b} Chiara Zanato,^a Benjamin C. Lewis,^b Pramod C. Nair,^b Sergio Dall'Angelo,^a Matteo Zanda*^{a,c} and Arduino A. Mangoni*^b

Dimethylarginine dimethylaminohydrolase (DDAH) is a key enzyme involved in the metabolism of asymmetric dimethylarginine (ADMA) and *N*-monomethyl arginine (NMMA), which are endogenous inhibitors of the nitric oxide synthase (NOS) family of enzymes. Two isoforms of DDAH have been identified in humans, DDAH-1 and DDAH-2. DDAH-1 inhibition represents a promising strategy to limit the overproduction of NO in pathological states without affecting the homeostatic role of this important messenger molecule. Here we describe the design and synthesis of 12 novel DDAH-1 inhibitors and report their derived kinetic parameters, IC₅₀ and K_i. Arginine analogue **10a**, characterized by an acylsulfonamide isosteric replacement of the carboxylate, showed a 13-fold greater inhibitory potential relative to the known DDAH-1 inhibitor, L-257. Compound **10a** was utilized to study the putative binding interactions of human DDAH-1 inhibition using molecular dynamics simulations. The latter suggests that several stabilizing interactions occur in the DDAH-1 active-site, providing structural insights for the enhanced inhibitory potential demonstrated by *in vitro* inhibition studies.

Received 3rd September 2015,
Accepted 22nd September 2015

DOI: 10.1039/c5ob01843a

www.rsc.org/obc

Introduction

Nitric Oxide (NO) and its related pathways represent an important target in medicinal chemistry not only due to its ability to act as a key physiological messenger and modulator, but also due to the growing evidence identifying its role in the onset and progression of several pathological states.¹ Under physiological conditions NO is synthesized in low, tightly regulated concentrations² in order to modulate a number of physiological functions, including: vascular tone and blood flow,³ platelet and leukocytes cell adhesion,^{4,5} and the long-term potentiation and mediation of behavioural activity.^{6,7} Impairment of NO synthesis is commonly associated with pulmonary and systemic hypertension,^{8,9} kidney disease,¹⁰ erectile dysfunction,¹¹ pre-eclampsia,¹² and cerebrovascular disease.¹³ By contrast, excessive NO concentrations are observed in cases of septic shock,¹⁴ migraine,¹⁵ pulmonary fibrosis,¹⁶ inflammatory

diseases,^{17,18} tumour angiogenesis,¹⁹ and neurodegenerative disorders.²⁰

NO is synthesized through a five-electron oxidative reaction catalyzed by one of the three nitric oxide synthase isoforms (nNOS, eNOS and iNOS), each with varying tissue distribution.^{21,22} Utilizing NADPH and molecular oxygen (O₂), NO is harboured upon the conversion of endogenous L-arginine into L-citrulline (Fig. 1).^{23,24}

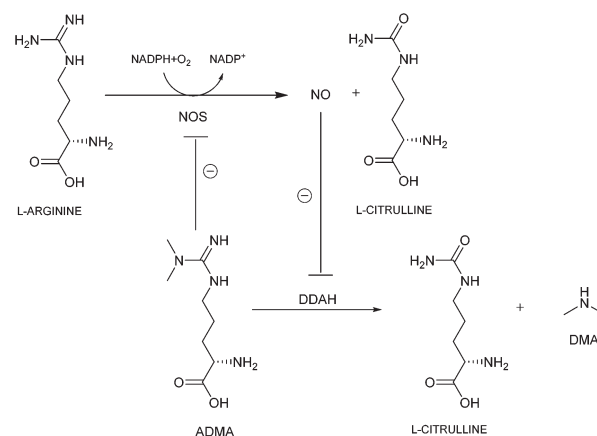


Fig. 1 Schematic diagram highlighting the overlap between DDAH and NOS biochemical pathways.

^aKosterlitz Centre for Therapeutics, Institute of Medical Sciences, School of Medical Sciences, University of Aberdeen, Aberdeen AB25 2ZD, UK.

E-mail: m.zanda@abdn.ac.uk

^bDepartment of Clinical Pharmacology, School of Medicine, Flinders University and Flinders Medical Centre, Bedford Park, SA 5042, Australia.

E-mail: arduino.mangoni@flinders.edu.au

^cC.N.R.-I.C.R.M., via Mancinelli 7, 20131 Milan, Italy

† Electronic supplementary information (ESI) available: Copies of ¹H, ¹⁹F and ¹³C NMR spectra for all the new compounds. See DOI: 10.1039/c5ob01843a

The methylated arginines, namely asymmetric dimethyl arginine (ADMA) and *N*-monomethyl arginine (NMMA), are competitive endogenous inhibitors of all three NOS isoforms (Fig. 1).²² ADMA and NMMA are released upon the proteolytic cleavage of proteins methylated by Type-1 protein arginine methyl transferases (PRMTs).²⁵ The metabolic clearance of ADMA and NMMA is primarily mediated by the dimethyl-arginine dimethylaminohydrolase (DDAH) family of enzymes which hydrolyse methylated arginines to *L*-citrulline and dimethylamine, or monomethylamine, respectively.^{1,26} Two DDAH isoforms have been identified in humans, DDAH-1 and DDAH-2, which share approximately 62% protein sequence homology yet vary in terms of their tissue distribution.²⁷ Both are reported to require chelation with Zn²⁺ and are primarily localized to the cytoplasm, however a hydrophobic secondary motif additionally enables association with lipid membranes, such as the mitochondrial membrane.^{28,29}

DDAH-1 is primarily associated with the metabolism of ADMA and NMMA, whereas the biochemical role of DDAH-2 remains unclear. Moreover, literature reports suggest that methylated arginines are not DDAH-2 substrates.³⁰

Since DDAH plays a key role in the regulation of NO concentrations *in vivo*, the modulation of its activity may represent a potential therapeutic approach in the treatment of pathological states associated with excessive NO production. As such, several classes of DDAH inhibitors have been described in the literature.³¹ Many exhibit moderately good inhibitory potential with selectivity primarily towards the bacterial isoenzyme PaDDAH, such as SR445 and pentafluorophenyl (PFP) sulphonates,^{32,33} whereas others are effective on the human DDAH (hDDAH), in particular L-VNIO, L-257 and the corresponding methyl ester, L-291 (Fig. 2).^{22,32}

The modification of both the guanidyl group and *N*-substituent of arginine-like hDDAH-1 inhibitors has been extensively explored as one strategy to improve their selectivity and phar-

macokinetic properties.^{32,34,35} Conversely, modifications of the carboxylic acid functional group have not been extensively investigated.³⁴ Here we report the synthesis and characterization of a number of arginine analogues incorporating bioisosteric replacements of the carboxylic acid functional group and reveal they act as potent inhibitors of recombinant hDDAH-1.

Results and discussion

Inhibitor design and synthesis

Among the hDDAH-1 inhibitors reported to date, L-257 displayed the highest selectivity for hDDAH-1, with no inhibitory effect on the NOS and arginase families of enzymes.^{34,36} Due to these favourable characteristics, the chemical scaffold of L-257 was adopted for the synthesis of a small library of two different classes of novel potential hDDAH-1 inhibitors:³⁶ L-257 side-chain derivatives and L-257 carboxylate bioisosteres. 1,2,3-Triazoles structurally unrelated with L-257 were also investigated in this work.

L-257 side-chain derivatives

Initial modifications introduced alterations to the side-chain, as in compounds **3a-f** (Scheme 1), which were obtained from the commercially available carboxamide **2** and the corresponding alcohols **1a-f** under Mitsunobu conditions,³⁷ using DIAD and Ph₃P in THF. Products **3a-f** were isolated in 47–99% yields by column chromatography. Guanidination of Boc-Orn-O*t*Bu hydrochloride **4** with **3a-f** using DIPEA as a base and subsequent Boc-deprotection in TFA/DCM (1 : 1 v/v), gave the *N*-monoalkylated-*L*-arginines **6a-e** in 69–99% yields (Scheme 1).

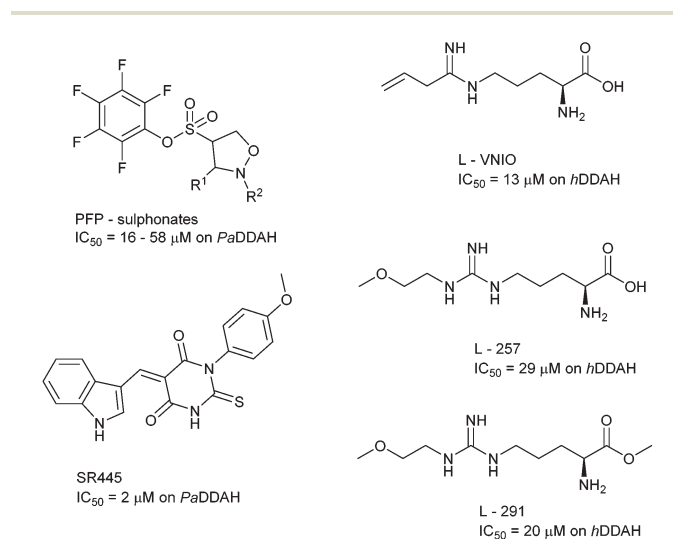
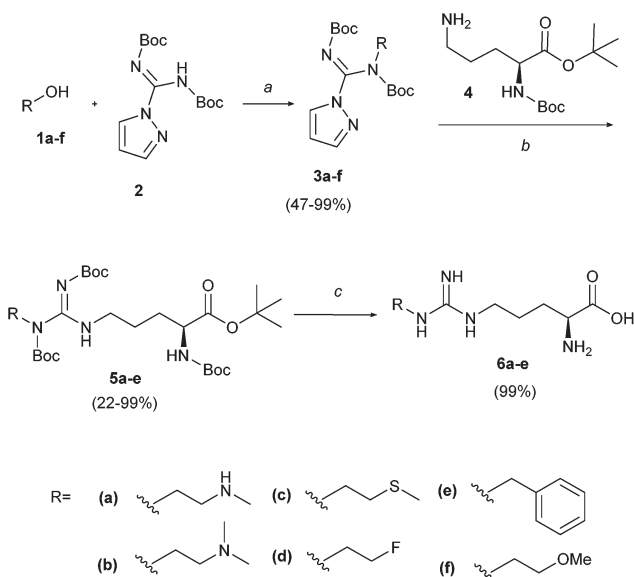
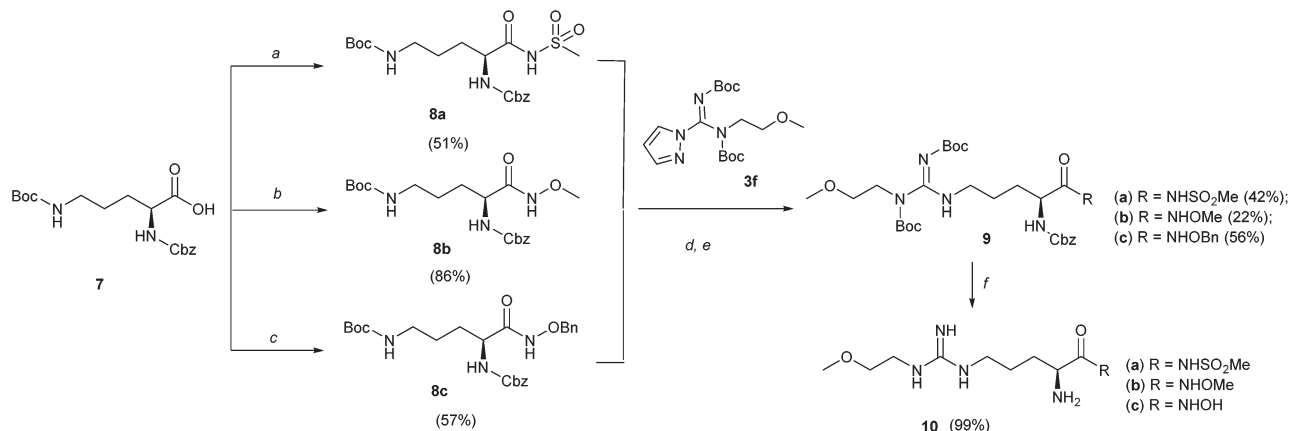


Fig. 2 Current DDAH inhibitors reported in the literature with their IC₅₀ values.^{22,32}



Scheme 1 L-257 side-chain derivatives synthesis. Reaction conditions: (a) Ph₃P, DIAD, THF, 0 °C-rt, 16 h, 47–99%; (b) DIPEA, DCM, rt, 24 h, 22–99%; (c) TFA, DCM, rt, 3 h, 99%.



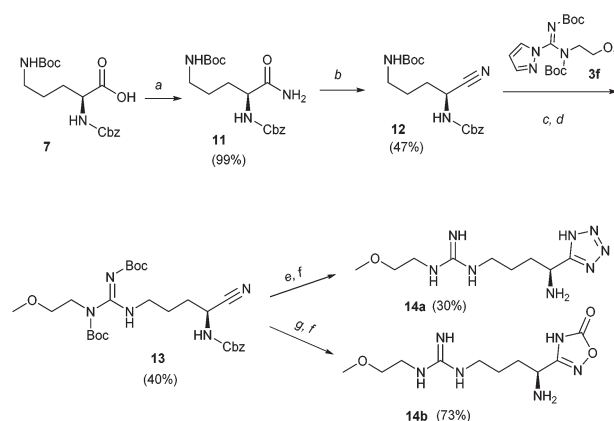
Scheme 2 L-257 linear bioisosteres synthesis. Reaction conditions: (a) CDI, DBU, methanesulfonamide, THF, rt, 7 h, 51%; (b) HATU, DIPEA, *O*-methylhydroxylamine hydrochloride, THF, 0 °C-rt, 16 h, 86%; (c) HATU, DIPEA, *O*-benzylhydroxylamine, THF, 0 °C-rt, 16 h, 57%; (d) HCl/dioxane (4 N), DCM, rt, 30 min, 99%; (e) DIPEA, DCM, rt, 24 h, 22–99%; (f) TFA, TFMSA, rt, 1 h, 99%.

To investigate the effect of side-chain alteration at the 2-methoxyethyl end of the L-257 scaffolds, five compounds **6a–e** were synthesized bearing diverse substituents. In compound **6a** a 2-(methylamino)ethyl group was introduced to determine the effect of substituting the oxygen with nitrogen. To determine the effect of a modified terminal amino group, compound **6b** carrying a 2-(dimethylamino)ethyl side-chain was designed. Furthermore, to explore the role of hydrophobic interactions and π -stacking in hDDAH-1 inhibition, compound **6c** with a 2-(methylthio)ethyl group and compound **6e** bearing a 3-benzylguanidino substituent were designed, respectively. Finally, compound **6d** incorporated a 2-fluoroethyl side-chain to investigate the impact of altered electronegativity.

L-257 bioisosteres

Analogues **10a–c** (Scheme 2) and **14a,b** (Scheme 3) originated from bioisosteric replacement of the carboxylate group on the L-257 scaffold.³⁸ Compound **10a** was designed by replacing the carboxylate with a methyl sulfonimide. The overall geometrical topology and acidity of methyl sulfonimides are similar to the carboxylate,³⁹ however they are metabolically more resistant,⁴⁰ with the potential to form strong polar interactions within the hDDAH-1 active-site.³⁹ Compounds **10b** and **10c** are the corresponding *O*-methyl-hydroxamate and hydroxamate analogues of L-257, respectively. These modifications were introduced to investigate the effect of decreasing the acidity of the carboxylate group by substitution with a functional group characterized by a higher pK_a (8–9).⁴¹ Z-Orn(Boc)-OH **7** (Scheme 2) was used as starting material for the synthesis of **10a–c**. Deprotection of the side-chain Boc-amino group using a solution of HCl (4 N) in 1,4-dioxane⁴² and guanidination with **3f**, followed by full deprotection of the resulting derivatives **9a–c** afforded the desired products **10a–c** in 22–56% yields.

Analogues **14a** and **14b** (Scheme 3) incorporated azole bioisosteric groups and were produced from the corresponding primary amide **11** and the nitrile **12** – obtained by TFAA-pro-



Scheme 3 Azole bioisosteres synthesis. Reaction conditions: (a) ^tBuCOCl, *N*-methylmorpholine, NH₄OH (30%), THF, –10 °C-rt, 3 h, 99%; (b) TFAA, TEA, THF, 0 °C-rt, 16 h, 47%; (c) HCl/dioxane (4 N), DCM, rt, 30 min, 99%; (d) DIPEA, DCM, rt, 24 h, 22–99%; (e) NaN₃, ZnBr₂, water/2-propanol, reflux, 16 h, 30%; (f) TFA, DCM, rt, 3 h, 99% (g) (1) NH₂OH·HCl, NaHCO₃, DMSO, reflux, 16 h; (2) CDI, DBU, THF, reflux, 30 min, 73%.

motated dehydration – using Z-Orn(Boc)-OH **7** as starting material. The guanidine group was introduced after cleavage of the side-chain *N*-Boc group of **12**, followed by reaction with the same Mitsunobu product **3f** (Scheme 1) used to synthesize L-257.³⁴ The resulting nitrile derivative **13** was reacted with sodium azide according to the procedure described by Demko and Sharpless.⁴³ The resulting tetrazole was fully deprotected using TFA and TFMSA, affording compound **14a**. The nitrile **13** was also converted into the 5-oxo-1,2,4-oxadiazole derivative using hydroxylamine hydrochloride.⁴⁴ Final guanidine deprotection with TFA provided the free oxadiazolone product **14b**.

The rationale for introducing a tetrazole ring to generate compound **14a** was to replace the carboxylic acid function with a bioisostere having similar acidity (pK_a 4.5–4.9).⁴⁵ This substi-

tution is known to exhibit a 10-fold increase in lipophilicity, greater metabolic resistance,⁴⁶ and higher number of hydrogen bond acceptors. Alternatively, the 5-oxo-1,2,4-oxadiazole functional group (compound **14b**) exhibits reduced acidity (pK_a 6–7)⁴⁷ and increased lipophilicity,⁴⁸ relative to the carboxylate group.

1,2,3-Triazoles

The 1,2,3-triazoles **19** and **24** (Scheme 4), were synthesized utilizing Cu^I-catalyzed click chemistry.⁴⁹ The rationale for generating these triazoles is based on the work of Linsky and Fast,⁵⁰ who identified 4-halopyridines and benzimidazoles as key functions for the development of novel DDAH inhibitors, although **19** and **24** are structurally unrelated to ADMA and NMMA. Interestingly, in the PaDDAH active-site, the 4-halopyridines exhibited covalent binding at the enzyme's catalytic cysteine, whereas the benzimidazoles were shown to be weak reversible inhibitors, occupying a region of the active-site usually accommodating the substrate's side-chain. We therefore hypothesized that connecting these two functions through a triazole linker may improve the inhibitory potential of the resulting compounds. Compound **19** was synthesized by cycloaddition between the alkyne **18**, obtained by Sonogashira C–C coupling from 2-bromo-4-chloropyridine **17**,⁵¹ and azide **16**, obtained from 1-*H*-benzimidazole-2-methanol **15** by reaction with diphenylphosphoryl azide⁵² (Scheme 4). Similarly, triazole **24** was synthesized by reacting the alkyne **21**, obtained from 2-bromo-1-*H*-benzimidazole **20** under Sonogashira conditions,⁵³ and azide **23** resulting from the reaction between 4-chloro-2-(hydroxymethyl)pyridine **22** and diphenylphosphoryl azide⁵² (Scheme 4).

hDDAH-1 inhibition

All the novel compounds described herein were assessed along with L-257 for their inhibitory potential against hDDAH-1. Recombinant hDDAH-1 was expressed in HEK293T cells

according to the procedure described by Lewis *et al.*⁵⁴ *In vitro* pharmacokinetic parameters of hDDAH-1 inhibition were derived by detecting L-citrulline formation *via* UPLC-MS⁵⁵ (see Experimental section).

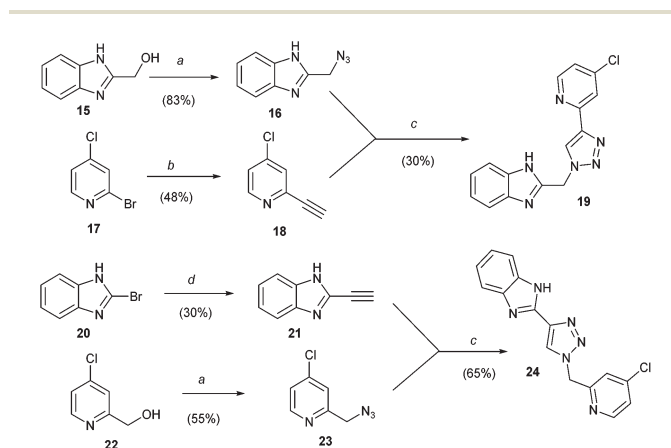
Inhibition experiments separately comprised each new compound and L-257 (0–1 mM) with ADMA (100 μ M) as the substrate. Reactions were initiated by the addition of pre-warmed substrate (37 °C) and allowed to incubate with shaking at 37 °C for 60 min. Deuterated d₆-L-citrulline (5 mg L⁻¹) was used as internal standard. Reactions were terminated by the addition of 200 μ L of ice-cold acetic acid 4% in methanol and prepared for analysis by diluting (3 : 10 v/v) in mobile phase. Incubation reactions utilized five concentrations of inhibitor (0, 0.1, 1, 10, 100 and 1000 μ M or 500 μ M) in screening studies and five concentrations in the range of 0–75 μ M in kinetic analyses.

Inhibition using the L-257 scaffold

In our hands, L-257 resulted in 83% inhibition at a concentration of 1 mM and the IC₅₀ value was calculated to be 31 μ M, with a K_i of 13 μ M.

Inhibition using L-257 side-chain derivatives

Modification of the L-257 methoxyethyl side-chain reduced the inhibitory potential (Table 1). Interestingly, three derivatives (**6c–e**) gave significant inhibition at concentrations of 1 mM, yet none resulted in low IC₅₀ values. The best inhibitors of this category were compounds **6c** and **6d** in which the methoxy group of L-257 was substituted with a methylthio and a fluorine group, respectively. Compound **6c** induced 80% of inhibition at 1 mM, relative to control experiments, and resulted in an IC₅₀ of 408 μ M. The IC₅₀ value for **6d** was calculated to be 379 μ M, with a percent inhibition of 67% at 1 mM (Table 1).



Scheme 4 Triazoles synthesis. (a) DPPA, DBU, toluene, rt, 16 h, 55–85%; (b) (Ph₃P)₂PdCl₂, CuI, TEA, ethynylTMS, 80 °C, 20 h, 48%; (c) CuI, sodium ascorbate, TEA, DCM, rt, 24 h, 30–65%; (d) (Ph₃P)₂PdCl₂, CuI, TEA, TIPS-acetylene, DMF, 80 °C, 72 h, 30%.

Table 1 Inhibitory potentials of the L-257 side-chain derivatives

Compound	R-	Inhibition at 1 mM (%)	IC ₅₀ (μ M)
6a		29	—
6b		14	—
6c		80	408 ± 19
6d		67	379 ± 5
6e		55	866 ± 3

Inhibition using 1,2,3-triazoles

Low inhibitory potential was observed with the two 1,2,3-triazoles **19** and **24** (Table 2). Both compounds were tested at the maximal concentration of 0.5 mM (instead of 1 mM), due to the poor solubility of these compounds. Compound **19** resulted in 9% inhibition at 0.5 mM and the IC_{50} value for this molecule was therefore not determined. Compound **24** exhibited greater inhibitory potential with an IC_{50} of 422 μ M and 57% inhibition at 0.5 mM.

Inhibition using L-257 bioisosteres

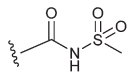
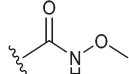
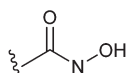
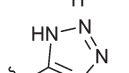
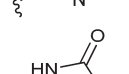
Interestingly, a different trend was observed with L-257 carboxylate bioisosteres (Table 3). Significantly enhanced inhibitory potential was exhibited by the acylsulfonamide **10a**

Table 2 Inhibitory potentials of the 1,2,3-triazoles

Compound	Inhibition at 0.5 mM (%)	IC_{50} (μ M)
19 ^a	9	—
24 ^a	57	422 \pm 4

^a Poor solubility at 1 mM.

Table 3 Inhibitory potentials of the L-257 bioisosteres

Compound	R-	Inhibition at 1 mM (%)	IC_{50} (μ M)	K_i (μ M)
10a		98	3 \pm 3	1 \pm 0
10b		79	230 \pm 2	—
10c		84	131 \pm 6	—
14a		91	34 \pm 7	14 \pm 1
14b		95	18 \pm 7	7 \pm 1

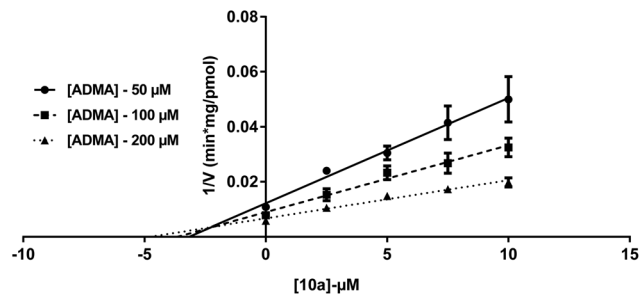


Fig. 3 Dixon plot of **10a** inhibition of L-citrulline formation by DDAH-1: experimentally determined values (points), model fitted curves of the best fit (lines).

that reduced L-citrulline formation of 98% at a concentration of 1 mM, relative to control experiments. The IC_{50} value determined for this compound was 3 μ M. Additionally, the oxadiazolone **14b** was also found to be effective, with 95% inhibition at a concentration of 1 mM. The IC_{50} value derived for this bioisostere was 18 μ M.

Compound **14a** exhibited 91% inhibition at a concentration of 1 mM, relative to control experiments, and its derived IC_{50} value was 34 μ M. Thus, although **14a** was less potent than **10a** and **14b**, it was still essentially equipotent to the reference compound, L-257.

Noteworthy, the inhibitory potential of these L-257 analogues was significantly decreased when the bioisosteric replacement was less acidic than the carboxylate, such as the hydroxamic group (compound **10b**) or the O-methyl-hydroxamic group (compound **10c**). This suggests that electrostatic interactions with positively charged residues of the hDDAH-1 active-site may facilitate the inhibitor binding.

A more detailed study of the kinetics of inhibition using compound **10a** (Fig. 3) and **14a–b** with ADMA as the substrate showed agreement with the competitive model of inhibition with a K_i of 1 μ M, 14 μ M and 7 μ M, respectively.

Molecular dynamics simulations

To gain atomic-level insights into the mechanism of binding to hDDAH-1 we performed molecular dynamics (MD) simulations⁵⁶ on the most potent inhibitor, **10a**. A 50 ns MD simulation showed that inhibitor **10a** remains stable within the hDDAH-1 active-site, blocking the access of substrates to the catalytic cysteine (Cys273).

The X-ray structure of L-257 bound to hDDAH-1⁵⁷ identifies the hydrogen bonds involving the ligand's carboxamide nitrogen with the receptor's Asp72 side-chain and Leu29 main-chain oxygen atoms. These interactions are reproduced in the MD simulations of L-257 (data not shown). The same interactions are observed in the MD simulations of compound **10a** bound to hDDAH-1 (Fig. 4). Furthermore, the 2-methoxyethyl and the guanidine groups of compound **10a** show polar and hydrophobic interactions with the side-chains of Ser31, Glu77, Ser175, Asn220, and Leu270 and main chain atoms of Arg30, in analogy with the L-257 complex.

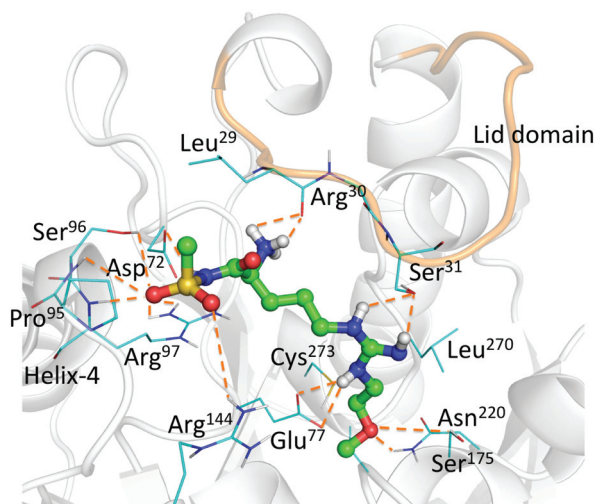


Fig. 4 The favoured binding mode of molecule **10a** (ball and stick) observed in molecular dynamics simulations (average configuration from 50 ns time scale). Green = carbon; red = oxygen; blue = nitrogen; yellow = sulphur. Only hydrogen atoms (white) involved in hydrogen bonds are shown for clarity. Hydrogen bonds are shown in dashed orange lines, with the 'lid' domain shown as a beige loop (residues 29–39). Secondary structure of DDAH-1 is rendered (cartoon).

Comparison of the X-ray crystal structure of hDDAH-1 bound to L-citrulline and L-257 shows that the Arg144 side-chain may adopt different conformational states, suggesting inhibitor-induced alterations within the hDDAH-1 active-site. In line with this observation, MD simulations with **10a** showed that the methyl sulfonamide group exploits a new binding region within the hDDAH-1 binding-site due to a reorganization of the Arg144 side-chain. The majority of interactions formed by the methyl sulfonamide group within this binding region are mediated *via* main-chain atoms of residues from helix 4. More specifically, one of the sulfonyl O atoms of compound **10a** forms four hydrogen bonds: with the main-chain NH of Pro95 and Ser96, with the side-chain OH of Ser96, and with the side-chain NH of Arg97. Interestingly, the first two interactions are not observed in hDDAH-1 bound to L-257 (neither in the crystal structure nor in MD simulations), and are the likely reason for the higher inhibitory potency of **10a** relative to L-257. The second oxygen of the sulfonyl group also acts as a hydrogen-bond acceptor with the side-chain NH of Arg144.

Crystal structures show that the 'lid' domain (loop region residues between 29 and 39) remains in an open state in the absence of inhibitor, however it adopts a closed conformation in the presence of an inhibitor.⁵⁷ One of the key interactions noted in the crystal structure in association to the lid domain is the hydrogen bonding interaction between the carboxamide NH of L-257 and the main-chain O atom of Leu29. The same hydrogen bonding interaction is observed in MD simulations of L-257 and compound **10a**. In addition to this interaction, MD simulations identify hydrophobic interactions between the methyl group of the methyl sulfonamide moiety of **10a** and the

side-chain atoms of Leu29 of the 'lid' domain. Such interactions further support closure of the 'lid' domain, thus corroborating the higher binding potential seen with compound **10a** *in vitro*.

Overall, the enhanced inhibitory effect of compound **10a** relative to L-257 is likely due to the network of hydrogen bonding interactions formed by the methyl sulfonamide group.

Conclusions

A total of 12 novel compounds were synthesized and tested for their ability to inhibit hDDAH-1. The kinetic parameters IC_{50} and K_i were measured. Three compounds: **10a**, **14a** and **14b**, demonstrated strong hDDAH-1 inhibitory potentials, which were higher or comparable to that of the best known inhibitor L-257. Compound **10a** ($K_i = 1 \mu\text{M}$; $IC_{50} = 3 \mu\text{M}$), incorporating an acylsulfonamide functional group, and compound **14b** ($K_i = 7 \mu\text{M}$; $IC_{50} = 18 \mu\text{M}$), carrying an oxadiazolone moiety, exhibited a 13-fold and 2-fold greater inhibitory potential, respectively, relative to L-257 ($K_i = 13 \mu\text{M}$; $IC_{50} = 31 \mu\text{M}$). The tetrazole substituted compound **14a** ($K_i = 14 \mu\text{M}$; $IC_{50} = 34 \mu\text{M}$) exhibited similar inhibitory activity to that of L-257. Owing to their complex synthetic pathways and inhibitory potentials similar to L-257, compound **14a–b** may not be ideal candidates for further development. Conversely, compound **10a** appears to be a promising hDDAH-1 inhibitor amenable to further structural modifications. MD simulations on this compound revealed that the methyl acylsulfonamide group is involved in a number of stabilizing interactions within the hDDAH-1 active-site, thus providing a mechanistic basis for the observed *in vitro* kinetic data.

Experimental section

Chemistry

^1H (400.13 MHz), ^{13}C (100.58 MHz) and ^{19}F (376.45 MHz) NMR spectra were recorded on a Bruker ADVANCE III spectrometer. For ^1H NMR spectra the solvent resonance was employed as the internal standard (CDCl_3 δ : 7.26, CD_3OD δ : 3.31, D_2O δ : 4.79, $(\text{CD}_3)_2\text{SO}$ δ : 2.50). ^{13}C NMR spectra were recorded with complete proton decoupling, and the solvent resonance was employed as the internal standard (CDCl_3 δ : 77.00, CD_3OD δ : 49.00, $(\text{CD}_3)_2\text{SO}$ δ : 39.52). ^{19}F NMR spectra were recorded with complete proton decoupling. The following abbreviations are used to describe spin multiplicity: s = singlet, d = doublet, t = triplet, m = multiplet, dd = doublet–doublet, dt = doublet–triplet, ddd = doublet–doublet–doublet, tt = triplet–triplet and br = broad signal. All chemical shifts (δ) are expressed in parts per million (ppm) and coupling constant (J) are given in Hertz (Hz). HPLC-MS experiments were performed on an Agilent Technologies 1200 Series HPLC system equipped with a DAD and a 6120 MS detector composed by a ESI ionization source and a Single Quadrupole

mass selective detector using a Analytical C18 RP column (Phenomenex Luna C18(2), 250 mm × 4.6 mm, 5 μm, 100 Å). HPLC purifications were performed on the Agilent 1260 system using a semi preparative C18 RP column (Phenomenex Luna, C18(2), 250 mm × 10.0 mm, 5 μm, 100 Å). Specific optical rotation measurements were performed on a PolAAR model 21 at 589 nm and the value were calculated based on the equation $[\alpha]_D^{20} = (100\alpha)/(lc)$ where the concentration c is in g per 100 mL and the path length l is 1 dm. All reactions were carried out in oven- or flame-dried glassware under nitrogen atmosphere, unless stated otherwise. All starting materials and reagents were commercially available and they were used as received. Tetrahydrofuran (THF) and dichloromethane (DCM) over molecular sieves and dry *N,N'*-dimethylformamide (DMF) and dimethylsulfoxide (DMSO) were purchased from Acros Organics and used without further purification. Reactions were magnetically stirred and monitored by TLC on silica gel (60 F254 pre-coated glass plates, 0.25 mm thickness). Visualization was accomplished by irradiation with a UV lamp and/or staining with a ceric ammonium molybdate or KMnO₄ solution. Flash chromatography were performed on silica gel (60 Å, particle size 0.040–0.062 mm).

L-257 side-chain derivatives

General method for Mitsunobu reaction (Procedure A). Diisopropyl azodicarboxylate (DIAD, 1.5 eq.) was added dropwise to a stirring solution of *N,N'*-bis-*tert*-butoxycarbonylpyrazole-1*H*-carboximidine (1 eq.), the proper alcohol (1–2 eq.) and triphenylphosphine (1.5 eq.) in THF (7 mL) at 0 °C. The reaction was stirred overnight at room temperature, concentrated in vacuum and purified by flash column chromatography to achieve the *N*-alkylated product **3a–f** as a colourless oils.

General method for guanidination (Procedure B). Boc-Orn-*Ort*Bu hydrochloride **4** (1 eq.) was dissolved in DCM (2 mL) and DIPEA (1.5 eq.) was added to the stirring suspension obtaining a velar solution. The desired guanilating reagent obtained with procedure A (1 eq.) was then added to the solution and the mixture was stirred for 24 hours at room temperature. After the addition of DCM (10 mL), the organic phase was washed with an aqueous solution of KHSO₄ (1 M, 2 × 10 mL), water (10 mL), brine (10 mL) and dried over anhydrous sodium sulphate. The solvent was completely evaporated and the residue was purified by flash column chromatography to achieve the guanidino *tert*-butyl ester **5a–e** as white foams.

General method for Boc- and *tert*-butyl deprotection (Procedure C). The final deprotection was achieved by stirring at room temperature for 3 hours a solution of the *tert*-butyl esters **5a–e** (1 eq.) in TFA/DCM (1 : 1, 4 mL). The TFA was completely evaporated under a compressed air flow, the deprotected product was washed with *n*-hexane and precipitated with diethyl ether. A further purification *via* RP-HPLC was required, achieving the desired products **6a–e** as foams in quantitative yield.

***tert*-Butyl *N*-{[(*tert*-butoxy)carbonyl][2-(methylamino)ethyl]-amino}(1*H*-pyrazol-1-yl)methylidene} carbamate, **3a**.** (Procedure A) Yield 75% (0.352 g), *R*_f 0.24 (*n*-hexane/AcOEt 80 : 20).

¹H NMR (400 MHz, CDCl₃) δ: 7.85 (br, 1H, ArH), 7.61 (br, 1H, ArH), 6.35 (br, 1H, ArH), 3.75 (br, 2H, CH₂), 3.50 (br, 2H, CH₂), 2.82 (s, 3H, CH₃), 1.40 (s, 9H, *t*Bu), 1.35 (s, 9H, *t*Bu), 1.19 (s, 9H, *t*Bu).

¹³C NMR (100 MHz, CDCl₃) δ: 157.4 (CO), 155.5 (CO), 152.2 (CO), 144.6 (CN₃), 142.8 (C_{Ar}), 130.0 (C_{Ar}), 108.9 (C_{Ar}), 82.9 (C*t*Bu), 82.3 (C*t*Bu), 79.6 (C*t*Bu), 47.4 (CH₂N), 46.4 (NCH₂), 34.6 (CH₃), 28.3 (*t*Bu), 27.9 (*t*Bu), 27.6 (*t*Bu).

ESI MS *m/z*: [M + Na]⁺ calcd for C₂₂H₃₇N₅NaO₆ 490.3, [M + H]⁺ calcd for C₂₂H₃₈N₅O₆ 468.3, found (relative intensity) 490.3 (100) [M + Na]⁺, 468.3 (50) [M + H]⁺.

***tert*-Butyl *N*-{[(*tert*-butoxy)carbonyl]imino}(1*H*-pyrazol-1-yl)-methyl}-*N*-[2-(dimethylamino)ethyl] carbamate, **3b**.** (Procedure A) Yield 47% (0.180 g), *R*_f 0.15 (*n*-hexane/AcOEt 80 : 20).

¹H NMR (400 MHz, CDCl₃) δ: 7.93 (s, 1H, ArH), 7.60 (d, *J* = 1.0 Hz, 1H, ArH), 6.31 (dd, *J* = 2.6, 1.6 Hz, 1H, ArH), 3.76 (t, *J* = 6.0 Hz, 2H, CH₂N), 2.53 (t, *J* = 6.5 Hz, 2H, NCH₂), 2.13 (s, 6H, 2 × CH₃N), 1.41 (s, 9H, *t*Bu), 1.18 (s, 9H, *t*Bu).

¹³C NMR (100 MHz, CDCl₃) δ: 157.6 (CO), 152.4 (CO), 144.7 (CN₃), 142.8 (C_{Ar}), 130.2 (C_{Ar}), 108.4 (C_{Ar}), 82.5 (C*t*Bu), 82.0 (C*t*Bu), 57.4 (CH₂N), 46.2 (NCH₂), 45.2 (2 × CH₃N), 27.9 (*t*Bu), 27.7 (*t*Bu).

ESI MS *m/z*: [M + H]⁺ calcd for C₁₈H₃₂N₅O₄ 382.3, found (relative intensity) 382.2 (100) [M + H]⁺.

***tert*-Butyl *N*-{[(*tert*-butoxy)carbonyl]imino}(1*H*-pyrazol-1-yl)-methyl}-*N*-[2-(methylsulfonyl)ethyl] carbamate, **3c**.** (Procedure A) Yield 42% (0.162 g), *R*_f 0.28 (*n*-hexane/AcOEt 90 : 10).

¹H NMR (400 MHz, CDCl₃) δ: 7.94 (s, 1H, ArH), 7.62 (d, *J* = 1.0 Hz, 1H, ArH), 6.36 (dd, *J* = 2.7, 1.6 Hz, 1H, ArH), 3.95–3.87 (m, 2H, CH₂N), 2.81–2.75 (m, 2H, SCH₂), 2.04 (s, 3H, CH₃S), 1.42 (s, 9H, *t*Bu), 1.20 (s, 9H, *t*Bu).

¹³C (100 MHz, CDCl₃) δ: 157.4 (CO), 152.2 (CO), 144.6 (CN₃), 143.0 (C_{Ar}), 130.1 (C_{Ar}), 108.9 (C_{Ar}), 82.8 (C*t*Bu), 82.3 (C*t*Bu), 47.5 (CH₂N), 32.2 (SCH₂), 27.9 (*t*Bu), 27.6 (*t*Bu), 15.0 (CH₃S).

ESI MS *m/z*: [M-2Boc + H]⁺ calcd for C₇H₁₃N₄S 185.1, [M-Boc + H]⁺ calcd for C₁₂H₂₁N₄O₂S 285.1 [M + H]⁺ calcd for C₁₇H₂₉N₄O₄S 385.2, [M + Na]⁺ calcd for C₁₇H₂₈N₄NaO₄S 407.2, [2M + Na]⁺ calcd for C₃₄H₅₆N₈NaO₈S₂ 791.4, found (relative intensity) 185.1 (100) [M-2Boc + H]⁺, 285.1 (32) [M-Boc + H]⁺, 385.3 (26) [M + H]⁺, 407.2 (27) [M + Na]⁺, 791.3 (25) [2M + Na]⁺.

***tert*-Butyl *N*-{[(*tert*-butoxy)carbonyl]imino}(1*H*-pyrazol-1-yl)-methyl}-*N*-(2-fluoroethyl)carbamate, **3d**.** (Procedure A) Yield 97% (0.345 g), *R*_f 0.44 (*n*-hexane/AcOEt 80 : 20).

¹H NMR (400 MHz, CDCl₃) δ: 7.94 (s, 1H, ArH), 7.68 (dd, *J* = 1.5, 0.6 Hz, 1H, ArH), 6.42 (dd, *J* = 2.8, 1.6 Hz, 1H, ArH), 4.67 (dt, *J*_{H-F} = 46.9 Hz, *J*_{H-H} = 5.2 Hz, 2H, FCH₂), 4.00 (dt, *J*_{H-F} = 23.5, *J*_{H-H} = 4.6 Hz, 2H, CH₂N), 1.49 (s, 9H, *t*Bu), 1.28 (s, 9H, *t*Bu).

¹³C (100 MHz, CDCl₃) δ: 157.3(CO), 152.3(CO), 144.4(CN₃), 143.3 (C_{Ar}), 130.0 (C_{Ar}), 109.0 (C_{Ar}), 83.2 (C*t*Bu), 82.5 (C*t*Bu), 81.2 (d, *J*_{C-F} = 169.5 Hz, FCH₂), 48.6 (d, *J*_{C-F} = 22.3 Hz, CH₂N), 27.9 (*t*Bu), 27.7 (*t*Bu).

¹⁹F NMR (376 MHz, CDCl₃) δ: -225.68 (tt, *J* = 46.9, *J* = 23.5, 1F).

ESI MS *m/z*: [M-2Boc + H]⁺ calcd for C₆H₁₀FN₄ 157.1, [M-Boc + H]⁺ calcd for C₁₁H₁₈FN₄O₂ 257.1 [M + H]⁺ calcd for

$C_{16}H_{26}FN_4O_4$ 357.2, $[M + Na]^+$ calcd for $C_{16}H_{25}FN_4NaO_4$ 379.1, $[2M + Na]^+$ calcd for $C_{32}H_{50}F_2N_8NaO_8$ 735.4, found (relative intensity) 157.1 (100) $[M-2Boc + H]^+$, 257.1 (33) $[M-Boc + H]^+$, 357.1 (10) $[M + H]^+$, 379.1 (81) $[M + Na]^+$, 735.3 (49) $[2M + Na]^+$.

tert-Butyl N-{{[benzyl]([tert-butoxycarbonyl]amino)}(1H-pyrazol-1-yl)methylidene} carbamate, 3e. (Procedure A) Yield 99% (0.398 g), R_f 0.42 (*n*-hexane/AcOEt 75 : 25).

1H NMR (400 MHz, $CDCl_3$) δ : 7.59–7.58 (m, 2H, ArH), 7.41–7.35 (m, 2H, ArH), 7.27–7.14 (m, 3H, ArH), 6.26 (dd, J = 2.7, 1.6 Hz, 1H, ArH), 4.85 (s, 2H, CH_2N), 1.39 (s, 9H, *t*Bu), 1.17 (s, 9H, *t*Bu).

^{13}C (100 MHz, $CDCl_3$) δ : 157.5 (CO), 152.5 (CO), 144.4 (CN₃), 142.9 (C_{Ar}), 136.6 (C_{Ar}), 129.9 (C_{Ar}), 128.6 (C_{Ar}), 128.5 (2 × C_{Ar}), 127.7 (2 × C_{Ar}), 108.7 (C_{Ar}), 83.1 (C*t*Bu), 82.3 (C*t*Bu), 52.2 (CH₂N), 27.9 (*t*Bu), 27.7 (*t*Bu).

ESI MS m/z : $[M + H]^+$ calcd for $C_{21}H_{29}N_4O_4$ 401.2, $[M + Na]^+$ calcd for $C_{21}H_{28}N_4NaO_4$ 423.2, $[2M + Na]^+$ calcd for $C_{42}H_{56}N_8NaO_8$ 823.4, found (relative intensity) 401.2 (21) $[M + H]^+$, 423.2 (39) $[M + Na]^+$, 823.4 (100) $[2M + Na]^+$.

tert-Butyl N-{{[[[tert-butoxycarbonyl]imino]}(1H-pyrazol-1-yl)-methyl](2-methoxyethyl)carbamate, 3f. (Procedure A) Yield 95% (0.349 g), R_f 0.35 (*n*-hexane/AcOEt 75 : 25).

1H NMR (400 MHz, $CDCl_3$) δ : 7.87 (s, 1H, ArH), 7.61 (d, J = 1.0 Hz, 1H, ArH), 6.33 (dd, J = 2.7, 1.6 Hz, 1H, ArH), 3.84 (m, 2H, CH_2N), 3.58 (t, J = 5.6 Hz, 2H, OCH₂), 3.20 (s, 3H, CH₃O), 1.42 (s, 9H, *t*Bu), 1.19 (s, 9H, *t*Bu).

^{13}C (100 MHz, $CDCl_3$) δ : 157.4 (CO), 152.3 (CO), 144.6 (CN₃), 142.9 (C_{Ar}), 129.9 (C_{Ar}), 108.6 (C_{Ar}), 82.6 (C*t*Bu), 82.1 (C*t*Bu), 69.9 (CH₂N), 58.3 (CH₃O), 47.6 (OCH₂), 27.8 (*t*Bu), 27.6 (*t*Bu).

ESI MS m/z : $[M + H]^+$ calcd for $C_{17}H_{29}N_4O_5$ 369.2, $[M + Na]^+$ calcd for $C_{17}H_{28}N_4NaO_5$ 391.2, $[2M + Na]^+$ calcd for $C_{34}H_{56}N_8NaO_{10}$ 759.4, found (relative intensity) 369.2 (50) $[M + H]^+$, 391.2 (74) $[M + Na]^+$, 759.4 (100) $[2M + Na]^+$.

tert-Butyl 8-(tert-butoxycarbonyl)-14-[[tert-butoxycarbonyl]amino]-9-[[tert-butoxycarbonyl]imino]-2,2,5-trimethyl-4-oxo-3-oxa-5,8,10-triazapentadecan-15-oate, 5a. (Procedure B) Yield 77% (0.532 g), R_f 0.25 (dichloromethane/methanol 98 : 2).

$[\alpha]_D^{20}$ = +6.00 (c 1.0, $CHCl_3$).

1H NMR (400 MHz, DMSO, 80 °C) δ : 7.88 (br, 1H, NH), 6.56 (br, 1H, NH), 3.88–3.79 (m, 1H, CH), 3.48 (t, J = 6.8 Hz, 2H, NCH₂), 3.35 (t, J = 6.8 Hz, 2H, CH₂N), 3.15 (br, 2H, NCH₂), 2.82 (s, 3H, CH₃N), 1.82–1.67 (m, 1H, CH₂), 1.67–1.54 (m, 3H, CH₂), 1.44 (s, 9H, *t*Bu), 1.43 (s, 9H, *t*Bu), 1.42 (s, 9H, *t*Bu), 1.41 (s, 18H, 2 × *t*Bu).

^{13}C NMR (100 MHz, DMSO, 80 °C) δ : 171.9 (2 × CO), 160.0 (CN₃), 155.7 (CO), 152.8 (2 × CO), 81.3 (C*t*Bu), 80.8 (C*t*Bu), 79.3 (C*t*Bu), 78.7 (C*t*Bu), 78.3 (C*t*Bu), 54.9 (CH), 47.6 (NCH₂), 45.3 (CH₂N), 42.4 (NCH₂), 34.8 (CH₃N), 29.0 (CH₂), 28.7 (*t*Bu), 28.6 (*t*Bu), 28.5 (*t*Bu), 28.4 (*t*Bu), 28.2 (*t*Bu), 25.3 (CH₂).

ESI MS m/z : $[M + H]^+$ calcd for $C_{33}H_{62}N_5O_{10}$ 688.4, found (relative intensity) 688.4 (100) $[M + H]^+$.

tert-Butyl 5-[2,3-bis(tert-butoxycarbonyl)-3-[2-(dimethylamino)ethyl]guanidino]-2-[[tert-butoxycarbonyl]amino]pentanoate, 5b. (Procedure B) Yield 97% (0.599 g), R_f 0.16 (dichloromethane/methanol 96 : 4).

$[\alpha]_D^{20}$ = +9.00 (c 1.0, $CHCl_3$).

1H NMR (400 MHz, $CDCl_3$) δ : 5.10 (d, J = 7.8 Hz, 1H, NH), 4.13 (br, 1H, CH), 3.60 (br, 2H, CH₂N), 3.25 (br, 2H, NCH₂), 2.49 (br, 2H, NCH₂), 2.26 (s, 6H, 2 × CH₃), 1.88–1.72 (m, 1H, CH₂), 1.66–1.52 (m, 3H, 2 × CH₂), 1.43 (s, 9H, *t*Bu), 1.42 (s, 18H, 2 × *t*Bu), 1.40 (s, 9H, *t*Bu).

^{13}C NMR (100 MHz, $CDCl_3$) δ : 171.5 (2 × CO), 155.3 (CN₃), 152.3 (2 × CO), 82.0 (2 × C*t*Bu), 79.6 (C*t*Bu), 78.8 (C*t*Bu), 58.4 (CH₂N), 53.6 (CH), 45.5 (NCH₂), 45.3 (2 × CH₃), 42.5 (NCH₂), 30.5 (CH₂), 28.3 (*t*Bu), 28.2 (*t*Bu), 28.1 (*t*Bu), 27.9 (*t*Bu), 24.8 (CH₂).

ESI MS m/z : $[M + H]^+$ calcd for $C_{29}H_{56}N_5O_8$ 602.4, $[M + Na]^+$ calcd for $C_{29}H_{55}N_5NaO_8$ 624.4, found (relative intensity) 602.4 (100) $[M + H]^+$, 624.4 (10) $[M + Na]^+$.

tert-Butyl 5-[2,3-bis(tert-butoxycarbonyl)-3-[2-(methylthio)ethyl]guanidino]-2-[[tert-butoxycarbonyl]amino]pentanoate, 5c. (Procedure B) Yield 99% (0.601 g), R_f 0.28 (*n*-hexane/eAcOEt 80 : 20).

$[\alpha]_D^{20}$ = –6.00 (c 1.0, MeOH).

1H NMR (400 MHz, $CDCl_3$) δ : 5.04 (d, J = 7.7 Hz, 1H, NH), 4.12 (s, 1H, CH), 3.80 (t, J = 6.8 Hz, 2H, SCH₂), 3.24 (br, 2H, NCH₂), 2.61 (t, J = 6.9 Hz, 2H, CH₂N), 2.03 (s, 3H, CH₃S), 1.84–1.71 (m, 1H, CH₂), 1.68–1.49 (m, 3H, 2 × CH₂), 1.42 (s, 9H, *t*Bu), 1.41 (s, 9H, *t*Bu), 1.40 (s, 9H, *t*Bu), 1.37 (s, 9H, *t*Bu).

^{13}C NMR (100 MHz, $CDCl_3$) δ : 171.4 (2 × CO), 155.3 (2 × CO), 152.9 (CN₃), 82.6 (C*t*Bu), 82.1 (C*t*Bu), 79.7 (C*t*Bu), 79.2 (C*t*Bu), 53.5 (CH), 46.1 (SCH₂), 43.5 (NCH₂), 33.1 (CH₂N), 30.3 (CH₂), 28.3 (*t*Bu), 28.2 (*t*Bu), 28.1 (*t*Bu), 28.0 (*t*Bu), 24.9 (CH₂), 15.0 (CH₃S).

ESI MS m/z : $[M + H]^+$ calcd for $C_{28}H_{53}N_4O_8S$ 605.4, $[M + Na]^+$ calcd for $C_{28}H_{52}N_4NaO_8S$ 627.4, found (relative intensity) 605.4 (100) $[M + H]^+$, 627.4 (10) $[M + Na]^+$.

tert-Butyl 5-[2,3-bis(tert-butoxycarbonyl)-3-(2-fluoroethyl)guanidino]-2-[[tert-butoxycarbonyl]amino]pentanoate, 5d. (Procedure B) Yield 99% (0.570 g), R_f 0.35 (*n*-hexane/AcOEt 80 : 20).

$[\alpha]_D^{20}$ = –9.00 (c 1.0, MeOH).

1H NMR (400 MHz, DMSO, 80 °C) δ : 4.54 (dt, J_{F-H} = 47.3 Hz, J_{H-H} = 5.4 Hz, 2H, FCH₂), 3.88–3.79 (m, 1H, CH), 3.66 (dt, J_{F-H} = 23.7 Hz, J_{H-H} = 5.4 Hz, 2H, CH₂N), 3.15 (t, J = 6.4 Hz, 2H, NCH₂), 1.78–1.68 (m, 1H, CH₂), 1.66–1.54 (m, 3H, CH₂), 1.44 (s, 9H, *t*Bu), 1.43 (s, 9H, *t*Bu), 1.41 (s, 18H, 2 × *t*Bu).

^{13}C NMR (100 MHz, $CDCl_3$) δ : 171.4 (2 × CO), 155.3 (2 × CO), 152.6 (CN₃), 82.7 (C*t*Bu), 82.0 (C*t*Bu), 81.9 (d, J_{F-C} = 168.7 Hz, FCH₂), 79.6 (C*t*Bu), 79.4 (C*t*Bu), 53.4 (CH), 48.0 (d, J_{F-C} = 20.0 Hz, CH₂N), 43.4 (NCH₂), 30.2 (CH₂), 28.3 (*t*Bu), 28.2 (*t*Bu), 28.1 (*t*Bu), 27.9 (*t*Bu), 24.9 (CH₂).

^{19}F NMR (376 MHz, DMSO) δ : –220.73 (tt, J = 47.9, 23.8 Hz).

ESI MS m/z : $[M + H]^+$ calcd for $C_{27}H_{50}FN_4O_8$ 577.4, found (relative intensity) 577.4 (100) $[M + H]^+$.

tert-Butyl 5-[3-benzyl-2,3-bis(tert-butoxycarbonyl)guanidino]-2-[[tert-butoxycarbonyl]amino]pentanoate, 5e. (Procedure B) Yield 69% (0.427 g), R_f 0.31 (*n*-hexane/AcOEt 50 : 50).

$[\alpha]_D^{20}$ = –4.00 (c 1.0, MeOH).

1H NMR (400 MHz, $CDCl_3$) δ : 7.28–7.12 (m, 6H, ArH, NH), 4.90 (br, 1H, NH), 4.78 (s, 2H, CH₂N), 4.01 (br, 1H, CH), 2.97 (br, 2H, NCH₂), 1.53–1.23 (m, 40H, 2 × CH₂, 4 × *t*Bu).

^{13}C NMR (100 MHz, CDCl_3) δ : 171.4 ($2 \times \text{CO}$), 155.3 (CN_3), 150.7 (CO), 149.6 (CO), 137.9 (C_{Ar}), 128.5 ($2 \times \text{C}_{\text{Ar}}$), 128.3 (C_{Ar}), 127.6 ($2 \times \text{C}_{\text{Ar}}$), 82.6 (CtBu), 82.0 (CtBu), 79.7 (CtBu), 79.3 (CtBu), 53.5 (CH), 50.9 (CH_2N), 43.4 (NCH_2), 30.1 (CH_2), 28.3 (tBu), 28.2 (tBu), 28.1 (tBu), 28.0 (tBu), 24.9 (CH_2).

ESI MS m/z : $[\text{M} + \text{H}]^+$ calcd for $\text{C}_{32}\text{H}_{53}\text{N}_4\text{O}_8$ 621.4, $[\text{M} + \text{Na}]^+$ calcd for $\text{C}_{32}\text{H}_{52}\text{N}_4\text{NaO}_8$ 643.4, found (relative intensity) 621.4 (100) $[\text{M} + \text{H}]^+$, 643.4 (10) $[\text{M} + \text{Na}]^+$.

2-Amino-5-(3-(2-(methylamino)ethyl)guanidino)pentanoic acid, 6a. (Procedure C) Yield 99% (0.452 g).

$[\alpha]_{\text{D}}^{20} = +8.89$ (c 1.1, MeOH).

^1H NMR (400 MHz, MeOD) δ : 7.76 (broad peak, 2H, NH_2), 6.46 (broad peak, 1H, NH), 4.01 (t, $J = 6.3$ Hz, 1H, CH), 3.63 (t, $J = 5.9$ Hz, 2H, CH_2N), 3.36–3.22 (m, 4H, $2 \times \text{NCH}_2$), 2.77 (s, 3H, CH_3N), 2.11–1.90 (m, 2H, CH_2), 1.90–1.69 (m, 2H, CH_2).

^{13}C NMR (100 MHz, MeOD) δ : 170.3 (CO), 156.3 (CN_3), 52.2 (CH), 47.4 (NCH_2), 40.5 (NCH_2), 37.6 (CH_2N), 32.4 (CH_3N), 27.3 (CH_2), 24.0 (CH_2).

ESI MS m/z : $[\text{M} + \text{H}]^+$ calcd for $\text{C}_9\text{H}_{22}\text{N}_5\text{O}_2$ 232.2, $[2\text{M} + \text{H}]^+$ calcd for $\text{C}_{18}\text{H}_{43}\text{N}_{10}\text{O}_4$ 463.3, found (relative intensity) 232.2 (100) $[\text{M} + \text{H}]^+$, 463.3 (10) $[2\text{M} + \text{H}]^+$.

HRMS calcd for $\text{C}_9\text{H}_{22}\text{N}_5\text{O}_2$: 232.1768, found: 232.1766.

2-Amino-5-(3-(2-(dimethylamino)ethyl)guanidino)pentanoic acid, 6b. (Procedure C) Yield 99% (0.581 g).

$[\alpha]_{\text{D}}^{20} = +9.12$ (c 0.4, MeOH).

^1H NMR (400 MHz, MeOD) δ : 3.98 (t, $J = 6.3$ Hz, 1H, CH), 3.68 (t, $J = 6.2$ Hz, 2H, CH_2N), 3.39 (t, $J = 6.2$ Hz, 2H, NCH_2), 3.35–3.24 (m, 2H, NCH_2), 2.96 (s, 6H, $2 \times \text{CH}_3\text{N}$), 2.08–1.92 (m, 2H, CH_2), 1.89–1.71 (m, 2H, CH_2).

^{13}C NMR (100 MHz, MeOD) δ : 170.6 (CO), 156.3 (CN_3), 55.4 (NCH_2), 52.3 (CH), 42.3 ($2 \times \text{CH}_3\text{N}$), 40.5 (NCH_2), 36.3 (CH_2N), 27.2 (CH_2), 24.0 (CH_2).

ESI MS m/z : $[\text{M} + \text{H}]^+$ calcd for $\text{C}_{10}\text{H}_{24}\text{N}_5\text{O}_2$ 246.2, $[\text{M} + \text{Na}]^+$ calcd for $\text{C}_{10}\text{H}_{23}\text{N}_5\text{NaO}_2$ 268.2, found (relative intensity) 246.2 (100) $[\text{M} + \text{H}]^+$, 268.1 (10) $[\text{M} + \text{Na}]^+$.

HRMS calcd for $\text{C}_{10}\text{H}_{24}\text{N}_5\text{O}_2$: 246.1925, found: 246.1923.

2-Amino-5-[3-(2-(methylthio)ethyl)guanidino]pentanoic acid, 6c. (Procedure C) Yield 99% (0.470 g).

$[\alpha]_{\text{D}}^{20} = +6.78$ (c 0.4, MeOH).

^1H NMR (400 MHz, D_2O) δ : 3.99–3.73 (m, 1H, CH), 3.37 (t, $J = 6.5$ Hz, 2H, CH_2N), 3.20 (dd, $J = 9.8, 6.8$ Hz, 2H, NCH_2), 2.68 (t, $J = 6.5$ Hz, 2H, SCH_2), 2.06 (s, 3H, CH_3S), 1.95–1.80 (m, 2H, CH_2), 1.74–1.54 (m, 2H, CH_2).

^{13}C NMR (100 MHz, D_2O) δ : 162.8 (CO), 155.8 (CN_3), 53.1 (CH), 40.4 (NCH_2), 40.0 (CH_2N), 32.3 (SCH_2), 27.1 (CH_2), 23.8 (CH_2), 14.1 (CH_3S).

ESI MS m/z : $[\text{M} + \text{H}]^+$ calcd for $\text{C}_9\text{H}_{21}\text{N}_4\text{O}_2\text{S}$ 249.1, found (relative intensity) 249.1 (100) $[\text{M} + \text{H}]^+$.

HRMS calcd for $\text{C}_9\text{H}_{21}\text{N}_4\text{O}_2\text{S}$: 249.1380, found: 249.1378.

2-Amino-5-[3-(2-fluoroethyl)guanidine]pentanoic acid, 6d. (Procedure C) Yield 98% (0.433 g).

$[\alpha]_{\text{D}}^{20} = +12.22$ (c 0.5, MeOH).

^1H NMR (400 MHz, D_2O) δ : 4.52 (dt, $J_{\text{H-F}} = 46.9$ Hz, $J_{\text{H-H}} = 4.7$ Hz, 2H, FCH_2), 3.96 (t, $J = 5.8$ Hz, 1H), 3.47 (dt, $J_{\text{H-F}} = 28.2$ Hz, $J_{\text{H-H}} = 4.7$ Hz, 2H, CH_2N), 3.20 (t, $J = 6.8$ Hz, 2H, NCH_2), 1.98–1.81 (m, 2H, CH_2), 1.77–1.53 (m, 2H, CH_2).

^{13}C (100 MHz, D_2O) δ : 172.2 (CO), 156.1 (CN_3), 82.6 (d, $J_{\text{C-F}} = 164.4$ Hz, FCH_2), 52.8 (CH), 41.6 (d, $J_{\text{C-F}} = 19.8$ Hz, CH_2N), 40.4 (NCH_2), 27.0 (CH_2), 23.8 (CH_2).

^{19}F NMR (376 MHz, D_2O) δ : -222.94 (tt, $J_{\text{H-F}} = 46.9$ Hz, $J_{\text{H-F}} = 28.1$ Hz, 1F, FCH_2).

ESI MS m/z : $[\text{M} + \text{H}]^+$ calcd for $\text{C}_8\text{H}_{18}\text{FN}_4\text{O}_2$ 221.1, found (relative intensity) 221.1 (100) $[\text{M} + \text{H}]^+$.

HRMS calcd for $\text{C}_8\text{H}_{18}\text{FN}_4\text{O}_2$: 221.1408, found: 221.1406.

2-Amino-5-(3-benzylguanidino)pentanoic acid, 6e. (Procedure C) Yield 98% (0.481 g).

$[\alpha]_{\text{D}}^{20} = +10.19$ (c 1.1, MeOH).

^1H NMR (400 MHz, D_2O) δ : 7.41–7.24 (m, 5H, ArH), 4.38 (s, 2H, CH_2N), 3.91 (t, $J = 6.2$ Hz, 1H, CH), 3.20 (t, $J = 6.7$ Hz, 2H, NCH_2), 1.91–1.73 (m, 2H, CH_2), 1.72–1.53 (m, 2H, CH_2).

^{13}C NMR (100 MHz, D_2O) δ : 172.3 (CO), 155.8 (CN_3), 136.2 (C_{Ar}), 129.0 ($2 \times \text{C}_{\text{Ar}}$), 127.9 (C_{Ar}), 126.8 ($2 \times \text{C}_{\text{Ar}}$), 52.9 (CH), 44.4 (CH_2N), 40.4 (NCH_2), 27.0 (CH_2), 23.8 (CH_2).

ESI MS m/z : $[\text{M} + \text{H}]^+$ calcd for $\text{C}_{13}\text{H}_{21}\text{N}_4\text{O}_2$ 265.2, found (relative intensity) 265.2 (100) $[\text{M} + \text{H}]^+$.

HRMS calcd for $\text{C}_{13}\text{H}_{21}\text{N}_4\text{O}_2$: 265.1659, found: 265.1657.

Bioisoteres of the L-257

General method for guanidination (Procedure D). The opportune intermediate **8a–c** or **12** (1 eq.) was dissolved in DCM (2 mL) and a solution of HCl in 1,4-dioxane (4 N, 2 mL) was added. The mixture was stirred at room temperature for 30 minutes and then the solvent was evaporated to dryness. The hydrochloric salt obtained was used crude and redissolved in DCM (2 mL) and the desired guanilating reagent **3f** (1 eq.) was added to the stirring suspension. DIPEA (1.5 eq.) was then added dropwise and in 3 different portions to the solution and the mixture was stirred for 24 hours at room temperature. After the addition of DCM (10 mL), the crude was washed with an aqueous solution of KHSO_4 (1 M, 2×10 mL), water (10 mL), brine (10 mL) and dried over anhydrous sodium sulphate. The solvent was completely evaporated and the crude was purified by flash column chromatography to achieve the guanidino compounds **9a–o** or **13** as a gluey foams.

General method for final deprotection (Procedure E). The final deprotection was achieved by stirring at room temperature for 1 hour a solution of compound **9a–c** (1 eq.), TFMSA (6 eq.) and TFA (2 mL). The TFA and TFMSA were completely evaporated under a compressed air flow, the deprotected product was washed with *n*-hexane and precipitated with diethyl ether. A further purification *via* RP-HPLC was required to obtain the desired products **10a–c** or **14a–b** as a foamy oils in quantitative yield.

Benzyl tert-butyl [5-(methylsulfonylamido)-5-oxopentane-1,4-diyl]dicarbamate, 8a. To a solution of Z-Orn(Boc)-OH **7** (1 eq.) in dry THF (10 mL), CDI (2 eq.) was added under nitrogen flow and the solution stirred for 1 hour at room temperature. DBU (1.5 eq.) and methane sulphonamide (1.5 eq.) were then added and the resulting mixture was stirred overnight at room temperature. The solvent was evaporated and the crude residue redissolved in DCM (10 mL) and washed with 5% citric acid (2×10 mL), water (10 mL) and brine (10 mL). The organic

phase was dried over anhydrous sodium sulphate and the solvent evaporated. The crude residue was purified by flash column chromatography (6% methanol in dichloromethane) achieving the desired product **8a** as a white foam.

Yield 51% (0.225 g), R_f 0.36 (dichloromethane/methanol 90 : 10).

$[\alpha]_D^{20} = +3.00$ (c 1.0, MeOH).

$^1\text{H NMR}$ (400 MHz, DMSO) δ : 11.86 (s, 1H, NH), 7.66 (d, $J = 7.5$ Hz, 1H, NH), 7.45–7.24 (m, 5H, ArH), 6.79 (t, $J = 5.4$ Hz, 1H, NH), 5.04 (s, 2H, CH₂), 4.10–3.93 (m, 1H, CH), 3.23 (s, 3H, CH₃), 2.99–2.82 (m, 2H, NCH₂), 1.71–1.57 (m, 1H, CH₂), 1.56–1.42 (m, 3H, 2 \times CH₂), 1.38 (s, 9H, *t*Bu).

$^{13}\text{C NMR}$ (100 MHz, DMSO) δ : 172.9 (CO), 156.5 (CO), 156.0 (CO), 137.3 (C_{Ar}), 128.8 (2 \times C_{Ar}), 128.3 (C_{Ar}), 128.2 (2 \times C_{Ar}), 77.9 (*Ct*Bu), 66.1 (CH₂), 55.1 (CH), 41.4 (CH₃), 39.4 (NCH₂), 28.9 (CH₂), 28.7 (*t*Bu), 26.5 (CH₂).

ESI MS m/z : [M-Boc + H]⁺ calcd for C₁₄H₂₂N₃O₅S 344.1, [M + Na]⁺ calcd for C₁₉H₂₉N₃NaO₇S 466.2, found (relative intensity) 344.1 (80) [M-Boc + H]⁺, 466.1 (100) [M + Na]⁺.

Benzyl tert-butyl [5-(methoxyamino)-5-oxopentane-1,4-diyl]-dicarbamate, 8b. To a solution of Z-Orn(Boc)-OH **7** (1 eq.) in dry THF (1.5 mL) at 0 °C, HATU (1 eq.) and DIPEA (2 eq.) were added and the solution, which immediately turned bright yellow, was stirred for 10 minutes at 0 °C and then added dropwise to a stirring solution of *O*-methylhydroxylamine hydrochloride (1 eq.) and DIPEA (2 eq.) in dry THF (1.5 mL) at room temperature. The resulting mixture was stirred overnight at room temperature, then the solvent was evaporated and the residue redissolved in DCM (10 mL), washed with 0.1 N HCl (10 mL), water (10 mL) and brine (10 mL). The organic phase was dried over anhydrous sodium sulphate and the solvent evaporated achieving a white residue which was used directly in the next step, without further purification.

Yield 86% (0.470 g), R_f 0.26 (dichloromethane/methanol 95 : 5).

$^1\text{H NMR}$ (400 MHz, CDCl₃) δ 10.33 (br, 1H, NH), 7.41–7.23 (m, 5H, ArH), 6.02 (br, 1H, NH), 5.17–4.93 (m, 3H, NH, CH₂), 4.24 (br, 1H, CH), 3.70 (s, 3H, OCH₃), 3.28–2.97 (m, 2H, NCH₂), 1.83–1.61 (m, 2H, CH₂), 1.58–1.47 (m, 2H, CH₂), 1.41 (s, 9H, *t*Bu).

$^{13}\text{C NMR}$ (100 MHz, CDCl₃) δ 169.5 (CO), 156.7 (CO), 156.4 (CO), 136.2 (C_{Ar}), 128.5 (2 \times C_{Ar}), 128.1 (C_{Ar}), 127.9 (2 \times C_{Ar}), 79.4 (*Ct*Bu), 67.0 (CH₂), 64.1 (OCH₃), 51.4 (CH), 39.2 (NCH₂), 30.0 (CH₂), 28.4 (*t*Bu), 26.1 (CH₂).

ESI MS m/z : [M + Na]⁺ calcd for C₁₉H₂₉N₃NaO₆ 418.2, found (relative intensity) 418.2 (100) [M + Na]⁺.

Benzyl tert-butyl [5-[(benzyloxy)amino]-5-oxopentane-1,4-diyl]dicarbamate, 8c. To a solution of Z-Orn(Boc)-OH **7** (1 eq.) in dry THF (1.5 mL) at 0 °C, HATU (1 eq.) and DIPEA (2 eq.) were added and the solution, which immediately turned bright yellow, was stirred for 10 minutes at 0 °C and then added dropwise to a stirring solution of *O*-benzylhydroxylamine hydrochloride (1 eq.) and DIPEA (2 eq.) in dry THF (1.5 mL) at room temperature. The resulting mixture was stirred overnight at room temperature, then the solvent was evaporated and the

residue redissolved in DCM (10 mL) washed with 0.1 N HCl (10 mL), water (10 mL) and brine (10 mL). The organic phase was dried over anhydrous sodium sulphate and the solvent evaporated achieving a white residue which was used directly in the next step, without further purification.

Yield 57% (0.269 g), R_f 0.36 (dichloromethane/methanol 96 : 4).

$^1\text{H NMR}$ (400 MHz, DMSO, 80 °C) δ : 10.88 (s, 1H, NH), 7.46–7.24 (m, 10H, ArH), 6.97 (s, 1H, NH), 6.35 (s, 1H, NH), 5.06 (s, 2H, CH₂), 4.81 (s, 2H, CH₂), 3.94 (br, 1H, CH), 2.9 (dd, $J = 12.8, 6.7$ Hz, 2H, NCH₂), 1.68–1.54 (m, 2H, CH₂), 1.49–1.35 (m, 11H, CH₂, *t*Bu).

$^{13}\text{C NMR}$ (100 MHz, DMSO) δ : 169.2 (CO), 156.3 (CO), 156.0 (CO), 137.5 (C_{Ar}), 136.3 (C_{Ar}), 129.3 (4 \times C_{Ar}), 128.8 (C_{Ar}), 128.7 (C_{Ar}), 128.2 (2 \times C_{Ar}), 128.1 (2 \times C_{Ar}), 77.9 (*Ct*Bu), 77.3 (CH₂), 65.9 (CH₂), 52.7 (CH), 40.7 (NCH₂), 29.7 (CH₂), 28.7 (*t*Bu), 26.5 (CH₂).

ESI MS m/z : [M + Na]⁺ calcd for C₂₅H₃₃N₃NaO₆ 494.2, found (relative intensity) 494.2 (100) [M + Na]⁺.

Benzyl {10-[(tert-butoxycarbonyl)amino]-11-(2-methoxyethyl)-14,14-dimethyl-2,2-dioxido-4,12-dioxo-13-oxa-21⁶-thia-3,9,11-triazapentadec-9-en-5-yl}carbamate, 9a. (Procedure D) Yield 42% (0.271 g), R_f 0.4 (dichloromethane/methanol 95 : 5).

$[\alpha]_D^{20} = +2.50$ (c 0.8, MeOH).

$^1\text{H NMR}$ (400 MHz, DMSO) δ : 7.76–7.73 (m, 1H, NH), 7.41–7.27 (m, 5H, ArH), 6.91 (br, 1H, NH), 5.02 (s, 2H, CH₂), 3.84 (br, 1H, CH), 3.43 (br, 4H, OCH₂, CH₂N), 3.24 (s, 3H, CH₃O), 3.09 (br, 2H, NCH₂), 2.89 (s, 3H, CH₃), 1.75–1.61 (m, 1H, CH₂), 1.58–1.45 (m, 3H, CH₂), 1.39 (s, 9H, *t*Bu), 1.38 (s, 9H, *t*Bu).

$^{13}\text{C NMR}$ (100 MHz, DMSO) δ : 167.4 (CO), 156.1 (2 \times CO), 152.5 (CO, CN₃), 137.6 (C_{Ar}), 128.8 (2 \times C_{Ar}), 128.2 (C_{Ar}), 128.1 (2 \times C_{Ar}), 81.0 (*Ct*Bu), 78.0 (*Ct*Bu), 70.3 (CH₂N), 65.7 (CH₂), 58.5 (CH₃O), 56.3 (CH), 47.1 (OCH₂), 40.8 (NCH₂), 39.4 (CH₃), 30.4 (CH₂), 28.4 (*t*Bu), 28.3 (*t*Bu), 25.0 (CH₂).

ESI MS m/z : [M + H]⁺ calcd for C₂₈H₄₆N₅O₁₀S 644.3, found (relative intensity) 644.3 (100) [M + H]⁺.

Benzyl {10-[(tert-butoxycarbonyl)amino]-11-(2-methoxyethyl)-14,14-dimethyl-4,12-dioxo-2,13-dioxo-3,9,11-triazapentadec-9-en-5-yl}carbamate, 9b. (Procedure D) Yield 22% (0.132 g), R_f 0.3 (dichloromethane/methanol 95 : 5).

$[\alpha]_D^{20} = +1.33$ (c 1.5, MeOH).

$^1\text{H NMR}$ (400 MHz, DMSO) δ : 11.24 (s, 1H, NH), 7.54–7.50 (m, 1H, NH), 7.41–7.26 (m, 5H, ArH), 5.03 (s, 2H, CH₂), 3.87–3.78 (m, 1H, CH), 3.43 (br, 4H, OCH₂, CH₂N), 3.24 (s, 3H, CH₃O), 3.10 (br, 2H, NCH₂), 2.70 (s, 3H, OCH₃), 1.70–1.45 (m, 4H, 2 \times CH₂), 1.39 (s, 9H, *t*Bu), 1.38 (s, 9H, *t*Bu).

$^{13}\text{C NMR}$ (100 MHz, DMSO) δ : 168.8 (CO), 156.3 (2 \times CO), 152.5 (CO, CN₃), 137.4 (C_{Ar}), 128.8 (2 \times C_{Ar}), 128.3 (C_{Ar}), 128.2 (2 \times C_{Ar}), 79.7 (*Ct*Bu), 78.1 (*Ct*Bu), 70.3 (OCH₂), 65.9 (CH₂), 58.5 (CH₃O), 52.6 (CH), 47.1 (CH₂N), 41.7 (NCH₂), 38.7 (OCH₃), 29.6 (CH₂), 28.4 (*t*Bu), 28.3 (*t*Bu), 25.1 (CH₂).

ESI MS m/z : [M + H]⁺ calcd for C₂₈H₄₆N₅O₉ 596.3, found (relative intensity) 596.3 (100) [M + H]⁺.

Benzyl {10-[(tert-butoxycarbonyl)amino]-11-(2-methoxyethyl)-14,14-dimethyl-4,12-dioxo-1-phenyl-2,13-dioxo-3,9,11-

triazapentadec-9-en-5-yl}carbamate, 9c. (Procedure D) Yield 56% (0.376 g), R_f 0.36 (dichloromethane/methanol 95 : 5).

$$[\alpha]_D^{20} = -2.00 \text{ (} c \text{ 1.0, MeOH).}$$

$^1\text{H NMR}$ (400 MHz, DMSO) δ : 11.26 (s, 1H, NH), 7.57–7.48 (m, 1H, NH), 7.43–7.26 (m, 10H, ArH), 5.04 (s, 2H, CH₂), 4.79 (s, 2H, CH₂), 3.93–3.80 (m, 1H, CH), 3.43 (br, 4H, OCH₂, CH₂N), 3.23 (s, 3H, CH₃O), 3.09 (br, 2H, NCH₂), 1.67–1.42 (m, 4H, 2 × CH₂), 1.39 (s, 9H, *t*Bu), 1.37 (s, 9H, *t*Bu).

$^{13}\text{C NMR}$ (100 MHz, DMSO) δ : 169.1 (CO), 156.3 (2 × CO), 152.5 (CO, CN₃), 137.5 (C_{Ar}), 136.3 (C_{Ar}), 129.3 (4 × C_{Ar}), 128.8 (C_{Ar}), 128.7 (C_{Ar}), 128.3 (2 × C_{Ar}), 128.2 (2 × C_{Ar}), 81.1 (C*t*Bu), 78.1 (C*t*Bu), 77.3 (CH₂), 70.3 (CH₂N), 65.9 (CH₂), 58.5 (CH₃O), 52.7 (CH), 47.1 (OCH₂), 41.8 (NCH₂), 29.7 (CH₂), 28.4 (*t*Bu), 28.3 (*t*Bu), 25.0 (CH₂).

ESI MS m/z : [M + H]⁺ calcd for C₃₄H₅₀N₅O₉ 672.3, found (relative intensity) 672.3 (100) [M + H]⁺.

2-Amino-5-(3-(2-methoxyethyl)guanidino)-N-(methylsulfonyl)pentanamide, 10a. (Procedure E) Yield 99% (0.437 g).

$$[\alpha]_D^{20} = +3.54 \text{ (} c \text{ 2.5, MeOH).}$$

$^1\text{H NMR}$ (400 MHz, D₂O) δ : 3.94 (t, J = 6.0 Hz, 1H, CH), 3.53 (t, J = 5.0 Hz, 2H, CH₂N), 3.35–3.29 (m, 5H, OCH₂, CH₃), 3.25–3.15 (m, 5H, NCH₂, CH₃O), 1.98–1.84 (m, 2H, CH₂), 1.74–1.52 (m, 2H, CH₂).

$^{13}\text{C NMR}$ (100 MHz, D₂O) δ : 172.0 (CO), 156.2 (CN₃), 70.3 (CH₂N), 58.2 (CH₃), 54.0 (CH), 41.1 (OCH₂), 40.3 (NCH₂), 40.2 (CH₃O), 27.5 (CH₂), 23.4 (CH₂).

ESI MS m/z : [M + H]⁺ calcd for C₁₀H₂₄N₅O₄S 310.2, found (relative intensity) 310.1 (100) [M + H]⁺.

HRMS calcd for C₁₀H₂₄N₅O₄S: 310.1544, found: 310.1542.

2-Amino-N-methoxy-5-(3-(2-methoxyethyl)guanidino)pentanamide, 10b. (Procedure E) Yield 99% (0.088 g).

$$[\alpha]_D^{20} = +10.00 \text{ (} c \text{ 0.5, MeOH).}$$

$^1\text{H NMR}$ (400 MHz, D₂O) δ : 3.79 (t, J = 6.9 Hz, 1H, CH), 3.70 (s, 3H, OCH₃), 3.53 (t, J = 5.3 Hz, 2H, CH₂N), 3.32 (t, J = 5.3 Hz, 2H, OCH₂), 3.31 (s, 3H, CH₃O), 3.19 (t, J = 6.8 Hz, 2H, NCH₂), 1.92–1.77 (m, 2H, CH₂), 1.64–1.51 (m, 2H, CH₂).

$^{13}\text{C NMR}$ (100 MHz, D₂O) δ : 165.9 (CO), 156.2 (CN₃), 70.3 (CH₂N), 64.4 (OCH₃), 58.2 (CH₃O), 50.7 (CH), 41.1 (OCH₂), 40.3 (NCH₂), 27.7 (CH₂), 23.7 (CH₂).

ESI MS m/z : [M + H]⁺ calcd for C₁₀H₂₄N₅O₃ 262.2, found (relative intensity) 262.2 (100) [M + H]⁺.

HRMS calcd for C₁₀H₂₄N₅O₃: 262.1874, found: 262.1872.

2-Amino-N-hydroxy-5-(3-(2-methoxyethyl)guanidino)pentanamide, 10c. (Procedure E) Yield 99% (0.118 g).

$$[\alpha]_D^{20} = +14.10 \text{ (} c \text{ 0.8, MeOH).}$$

$^1\text{H NMR}$ (400 MHz, D₂O) δ : 3.79 (t, J = 7.0 Hz, 1H, CH), 3.53 (t, J = 5.0 Hz, 2H, CH₂N), 3.36–3.28 (m, 5H, OCH₂, CH₃O), 3.18 (t, J = 6.8 Hz, 2H, NCH₂), 1.94–1.77 (m, 2H, CH₂), 1.69–1.46 (m, 2H, CH₂).

$^{13}\text{C NMR}$ (100 MHz, D₂O) δ : 166.2 (CO), 156.2 (CN₃), 70.3 (CH₂N), 58.2 (CH₃O), 50.9 (CH), 41.1 (OCH₂), 40.4 (NCH₂), 27.8 (CH₂), 23.8 (CH₂).

ESI MS m/z : [M + H]⁺ calcd for C₉H₂₂N₅O₃ 248.2, found (relative intensity) 248.2 (100) [M + H]⁺.

HRMS calcd for C₉H₂₂N₅O₃: 248.1717, found: 248.1717.

Benzyl tert-butyl (5-amino-5-oxopentane-1,4-diyl)dicarbamate, 11. Z-Orn(Boc)-OH **7** (1 eq.) and *N*-methylmorpholine (1.1 eq.) were dissolved in THF (7 mL), the solution was cooled down to –10 °C. Isobutyl chloroformate (1.1 eq.) was added dropwise and the mixture was stirred for 20 minutes. An aqueous ammonia solution 30% (6 eq.) was then added and the reaction was allowed to warm to room temperature. After 1 h, AcOEt (10 mL) was, the mixture was washed with an aqueous HCl solution (1 N, 10 mL), water (10 mL), brine (10 mL) and dried over anhydrous sodium sulphate. The solvent was evaporated achieving compound **11** as a white powder which was used directly in the next step without further purification.

Yield 99% (0.375 g), R_f 0.35 (dichloromethane/methanol 95 : 5).

$^1\text{H NMR}$ (400 MHz, DMSO) δ : 7.40–7.22 (m, 7H, 5 × ArH, NH, NH₂), 6.98 (s, 1H, NH₂), 6.79 (t, J = 5.4 Hz, 1H, NH), 5.02 (s, 2H, CH₂), 3.94–3.87 (m, 1H, CH), 2.92–2.83 (m, 2H, NCH₂), 1.60 (br, 1H, CH₂), 1.55–1.40 (m, 3H, 2 × CH₂), 1.38 (s, 9H, *t*Bu).

$^{13}\text{C NMR}$ (100 MHz, DMSO) δ : 174.3 (CO), 156.4 (CO), 156.1 (CO), 137.6 (C_{Ar}), 128.8 (2 × C_{Ar}), 128.2 (C_{Ar}), 128.1 (2 × C_{Ar}), 77.9 (C*t*Bu), 65.8 (CH₂), 54.7 (CH), 39.8 (NCH₂), 29.8 (CH₂), 28.7 (*t*Bu), 26.6 (CH₂).

ESI MS m/z : [M + Na]⁺ calcd for C₁₈H₂₇N₃NaO₅ 388.2, found (relative intensity) 388.1 (100) [M + Na]⁺.

Benzyl tert-butyl (1-cyanobutane-1,4-diyl)dicarbamate, 12. A solution of **11** (1 eq.) and triethylamine (2.4 eq.) in dry THF (6 ml) was stirred under nitrogen at 0 °C for 5 minutes. Tri-fluoroacetic anhydride (1.2 eq.) was added dropwise and the mixture was stirred for 1 hour at 0 °C and then overnight at room temperature. The solvent was evaporated and the residue was dissolved in diethyl ether (10 mL). The organic layer was washed with 0.1 N HCl (10 mL), 0.1 N NaOH (10 mL), water (10 mL), brine (10 mL), dried over anhydrous sodium sulphate and the solvent evaporated. The residue was purified by flash column (30% AcOEt in *n*-hexane) achieving the desired product **12** as a colourless foamy oil.

Yield 47% (0.162 g), R_f 0.35 (*n*-hexane/AcOEt 60 : 40).

$$[\alpha]_D^{20} = -27.00 \text{ (} c \text{ 1.0, MeOH).}$$

$^1\text{H NMR}$ (400 MHz, CDCl₃) δ : 7.42–7.28 (m, 5H, ArH), 6.19 (br, 1H, NH), 5.12 (s, 2H, CH₂), 4.84 (br, 1H, NH), 4.67–4.50 (m, 1H, CH), 3.12 (br, 2H, NCH₂), 1.90–1.71 (m, 2H, CH₂), 1.71–1.52 (m, 2H, CH₂), 1.43 (s, 9H, *t*Bu).

$^{13}\text{C NMR}$ (100 MHz, CDCl₃) δ : 156.2 (CO), 155.5 (CO), 135.8 (C_{Ar}), 128.6 (2 × C_{Ar}), 128.4 (C_{Ar}), 128.2 (2 × C_{Ar}), 118.7 (CN), 79.5 (C*t*Bu), 67.5 (CH₂), 42.6 (CH), 39.5 (NCH₂), 30.2 (CH₂), 28.4 (*t*Bu), 26.2 (CH₂).

ESI MS m/z : [M + Na]⁺ calcd for C₁₈H₂₅N₃NaO₄ 370.2, found (relative intensity) 370.1 (100) [M + Na]⁺.

tert-Butyl N-{N'-[4-[(benzyloxy)carbonyl]amino]-4-cyanobutyl]-N-(tert-butoxycarbonyl)-N-(2-methoxyethyl)carbamiimidoyl}glycinate, 13. (Procedure D) Yield 40% (0.219 g), R_f 0.31 (*n*-hexane/AcOEt 50 : 50).

$$[\alpha]_D^{20} = -17.00 \text{ (} c \text{ 1.0, MeOH).}$$

$^1\text{H NMR}$ (400 MHz, DMSO) δ : 8.21 (d, J = 7.8 Hz, 1H, NH), 7.45–7.31 (m, 5H, ArH), 5.09 (s, 2H, CH₂), 4.61 (dd, J = 7.5 Hz,

$J = 7.5$ Hz, 1H, CH), 3.44 (br, 4H, OCH₂, CH₂N), 3.24 (s, 3H, CH₃O), 3.14 (br, 2H, NCH₂), 1.89–1.70 (m, 2H, CH₂), 1.69–1.52 (m, 2H, CH₂), 1.40 (s, 9H, *t*Bu), 1.38 (s, 9H, *t*Bu).

¹³C NMR (100 MHz, DMSO) δ : 155.9 (2 \times CO), 152.5 (CO, CN₃), 136.9 (C_{Ar}), 128.9 (2 \times C_{Ar}), 128.5 (C_{Ar}), 128.4 (2 \times C_{Ar}), 120.1 (CN), 81.1 (C*t*Bu), 78.1 (C*t*Bu), 70.3 (CH₂N), 66.6 (CH₂), 58.5 (CH₃O), 47.1 (OCH₂), 42.4 (CH), 40.6 (NCH₂), 29.6 (CH₂), 28.4 (*t*Bu), 28.3 (*t*Bu), 24.7 (CH₂).

ESI MS m/z : [M + H]⁺ calcd for C₂₇H₄₂N₅O₇ 548.3, [M + Na]⁺ calcd for C₂₇H₄₁N₅NaO₇ 570.3, found (relative intensity) 548.3 (100) [M + H]⁺, 570.3 (10) [M + Na]⁺.

1-[4-Amino-4-(1*H*-tetrazol-5-yl)butyl]-3-(2-methoxyethyl)guanidine, 14a. The guanidino nitrile **13** (1 eq.) was dissolved in water (10 mL) and 2-propanol (5 mL) then sodium azide (2 eq.) and zinc bromide (0.5 eq.) were added. The reaction was refluxed overnight, then the solvent evaporated and the residue was dissolved in TFA (2 mL) and TFMSA (12 eq.). The reaction was stirred for 1 hour at room temperature, the acids were evaporated under compressed air flow and the residue was purified by RP-HPLC, obtaining compound **14a** as white foam.

Yield 30% (0.043 g).

¹H NMR (400 MHz, D₂O) δ : 4.82 (1H, t, $J = 7.2$ Hz, CH), 3.51 (2H, t, $J = 4.9$ Hz, CH₂N), 3.36–3.26 (5H, m, OCH₂, CH₃O), 3.15 (2H, t, $J = 6.8$ Hz, NCH₂), 2.16–2.03 (2H, m, CH₂), 1.65–1.35 (2H, m, CH₂).

¹³C NMR (100 MHz, D₂O) δ : 156.1 (C_{Ar}, CN₃), 70.3 (CH₂N), 58.2 (CH₃O), 46.2 (CH), 41.1 (OCH₂), 40.2 (NCH₂), 29.2 (CH₂), 23.8 (CH₂).

ESI MS m/z : [M + H]⁺ calcd for C₉H₂₁N₈O 257.2, found (relative intensity) 257.2 (100) [M + H]⁺.

HRMS calcd for C₉H₂₁N₈O: 257.1833, found: 257.1832.

1-[4-Amino-4-(5-oxo-4,5-dihydro-1,2,4-oxadiazol-3-yl)butyl]-3-(2-methoxyethyl)guanidine, 14b. A mixture of sodium bicarbonate (7.5 eq.) and hydroxylamine hydrochloride (5 eq.) in DMSO (5 mL) was stirred at 40 °C for 30 minutes, the guanidino nitrile **13** (1 eq.) was added and the mixture stirred overnight at 90 °C. The reaction was then allowed to cool at room temperature, water (10 mL) was added and aqueous phase was extracted with AcOEt (3 \times 10 mL). The combined organic phases were washed with brine (10 mL), dried over anhydrous sodium sulphate and the solvent was evaporated. The residue was redissolved in THF (10 mL) and CDI (1.2 eq.) and DBU (1.2 eq.) were added. The reaction was stirred for 30 minutes at room temperature and then diluted with AcOEt (10 mL), washed with 1 N HCl (10 mL), water (10 mL) and brine (10 mL). The organic phase was dried over anhydrous sodium sulphate and the solvent was evaporated. The intermediate was dissolved in TFA (2 mL) and TFMSA (12 eq.) and the reaction was stirred for 1 hour at room temperature. All the acids were evaporated under compressed air flow and the residue was purified by RP-HPLC, obtaining compound **14b** as white foam.

Yield 73% (0.012 g).

¹H NMR (400 MHz, D₂O) δ : 4.50 (t, $J = 6.7$ Hz, 1H, CH), 3.52 (t, $J = 5.0$ Hz, 2H, CH₂N), 3.34–3.27 (m, 5H OCH₂, CH₃O), 3.19

(t, $J = 6.8$ Hz, 2H, NCH₂), 2.09–1.89 (m, 2H, CH₂), 1.69–1.57 (m, 2H, CH₂).

¹³C (100 MHz, D₂O) δ : 163.2 (CO), 158.2 (C_{Ar}), 156.2 (CN₃), 70.3 (OCH₂), 58.2 (CH₃O), 46.5 (CH), 41.1 (NCH₂), 40.2 (CH₂N), 27.5 (CH₂), 23.4 (CH₂).

ESI MS m/z : [M + H]⁺ calcd for C₁₀H₂₁N₆O₃ 273.2, [2M + H]⁺ calcd for C₂₀H₄₁N₁₂O₆ 545.3, found (relative intensity) 273.1 (100) [M + H]⁺, 545.3 (80) [2M + H]⁺.

HRMS calcd for C₁₀H₂₁N₆O₃: 273.1675, found: 273.1677.

Triazoles synthesis

General azide synthesis method (Procedure F). To a stirring solution of alcohol **15** or **22** (1 eq.) in toluene (5 mL), diphenylphosphoryl azide (1.2 eq.) and DBU (1.3 eq.) were added. The reaction was stirred overnight at room temperature, diluted with water (10 mL) and extracted with AcOEt (3 \times 10 mL). The combined organic phases were washed with brine (10 mL), dried over anhydrous sodium sulphate and the solvent evaporated. The residue was purified by flash column chromatography (20% AcOEt: *n*-hexane) to achieve the desired azide **16** or **23** respectively as a colourless oils.

[Synthesis and complete characterization of compound **18** and **21** was reported by Gijzen *et al.* (2013)⁵¹ and Zornik, D. *et al.* (2011),⁵³ respectively.]

General triazole synthesis method (Procedure G). The alkyne **18** or **21** (1 eq.) and the azide **16** or **23** (1 eq.) were dissolved in DCM (10 mL). Copper iodide (0.2 eq.), sodium ascorbate (2 eq.) and triethylamine (1 eq.) were added. The reaction was stirred for 24 hours at room temperature then a saturated solution of ammonium chloride was added (10 mL). After stirring for 5 minutes the mixture was extracted with DCM (3 \times 10 mL), washed with brine (10 mL), dried over anhydrous sodium sulphate and the solvent was evaporated. The residue was purified by flash column chromatography (2% methanol in dichloromethane) to achieve the desired product **19** or **24** respectively as white foams.

2-(Azidomethyl)-1*H*-benzo[d]imidazole 16. (Procedure F) Yield 83% (0.144 g), *R*_f 0.36 (*n*-hexane/AcOEt 70 : 30).

¹H NMR (400 MHz, CDCl₃) δ : 11.76 (s, 1H, NH), 7.55 (dd, $J = 6.0, 3.2$ Hz, 2H, 2 \times ArH), 7.21 (dd, $J = 6.1, 3.1$ Hz, 2H, 2 \times ArH), 4.66 (s, 2H, CH₂).

¹³C NMR (101 MHz, CDCl₃) δ : 149.1 (2 \times C_{Ar}), 138.4 (C_{Ar}), 123.2 (2 \times C_{Ar}), 115.4 (2 \times C_{Ar}), 48.4 (CH₂).

ESI MS m/z : [M + H]⁺ calcd for C₈H₈N₅ 174.1, found (relative intensity) 174.1 (100) [M + H]⁺.

2-[[4-(4-Chloropyridin-2-yl)-1*H*-1,2,3-triazol-1-yl]methyl]-1*H*-benzo[d]imidazole 19. (Procedure G) Yield 30% (0.092 g), *R*_f 0.27 (dichloromethane/methanol 95 : 5).

¹H NMR (400 MHz, DMSO) δ : 12.68 (br, 1H, NH), 8.81 (s, 1H, CH), 8.61 (d, $J = 5.3$ Hz, 1H, ArH), 8.08 (d, $J = 1.8$ Hz, 1H, ArH), 7.59–7.50 (m, 3H, 3 \times ArH), 7.25–7.14 (m, 2H, 2 \times ArH), 5.98 (s, 2H, CH₂).

¹³C NMR (100 MHz, DMSO) δ : 151.9 (2 \times C_{Ar}), 151.8 (C_{Ar}), 148.7 (C_{Ar}), 146.6 (C_{Ar}), 144.3 (2 \times C_{Ar}), 125.4 (CH), 123.5 (3 \times C_{Ar}), 122.6 (2 \times C_{Ar}), 119.7 (C_{Ar}), 48.1 (CH₂).

ESI MS m/z : $[M + H]^+$ calcd for $C_{15}H_{12}ClN_6$ 311.1, $[M + Na]^+$ calcd for $C_{15}H_{11}ClN_6Na$ 333.1, found (relative intensity) 311.1 (100) $[M + H]^+$, 333.1 (20) $[M + Na]^+$.

HRMS calcd for $C_{15}H_{11}ClN_6Na$: 333.0631, found: 333.0629.

2-(Azidomethyl)-4-chloropyridine 23. (Procedure F) Yield 55% (0.091 g), R_f 0.51 (*n*-hexane/AcOEt 70 : 30).

1H NMR (400 MHz, $CDCl_3$) δ : 8.41 (d, $J = 5.3$ Hz, 1H, ArH), 7.30 (d, $J = 1.6$ Hz, 1H, ArH), 7.22–7.14 (m, 1H, ArH), 4.42 (s, 2H, CH_2).

^{13}C NMR (100 MHz, $CDCl_3$) δ : 157.5 (C_{Ar}), 150.4 (C_{Ar}), 144.9 (C_{Ar}), 123.2 (C_{Ar}), 122.1 (C_{Ar}), 55.0 (CH_2).

ESI MS m/z : $[M + H]^+$ calcd for $C_6H_6ClN_4$ 169.0, found (relative intensity) 169.1 (100) $[M + H]^+$.

2-{1-[(4-Chloropyridin-2-yl)methyl]-1H-1,2,3-triazol-4-yl}-1H-benzo[d]imidazole 24. (Procedure G) Yield 65% (0.198 g), R_f 0.31 (dichloromethane/methanol 95 : 5).

1H NMR (400 MHz, DMSO) δ : 13.10 (br, 1H, NH), 8.86 (s, 1H, CH), 8.54 (d, $J = 5.3$ Hz, 1H, ArH), 7.69–7.60 (m, 2H, 2 \times ArH), 7.56 (dd, $J = 5.3, 2.0$ Hz, 1H, ArH), 7.53–7.48 (m, 1H, ArH), 7.27–7.14 (m, 2H, 2 \times ArH), 5.89 (s, 2H, CH_2).

^{13}C NMR (100 MHz, DMSO) δ : 157.0 (C_{Ar}), 151.5 (C_{Ar}), 144.9 (C_{Ar}), 144.2 (C_{Ar}), 144.1 (C_{Ar}), 140.0 (C_{Ar}), 134.8 (C_{Ar}), 125.8 (C_{Ar}), 124.0 (C_{Ar}), 123.1 (C_{Ar}), 123.0 (C_{Ar}), 122.1 (C_{Ar}), 119.2 (C_{Ar}), 112.0 (C_{Ar}), 54.4 (CH_2).

ESI MS m/z : $[M + H]^+$ calcd for $C_{15}H_{12}ClN_6$ 311.1, $[M + Na]^+$ calcd for $C_{15}H_{11}ClN_6Na$ 333.1, found (relative intensity) 311.1 (100) $[M + H]^+$, 333.1 (20) $[M + Na]^+$.

HRMS calcd for $C_{15}H_{12}ClN_6$: 311.0806, found: 311.0810.

Molecular biology

DDAH-1 cloning and expression. The hDDAH-1 coding sequence (CDS; NM_012137) was shuttled into the pEF-IRES(6) mammalian expression vector. Cells were transfected with the pEF-IRES-DDAH-1 expression construct (4 μ g) using Lipofectamine2000 in OptiMEM (Invitrogen, CA, USA). The stable expression of hDDAH-1 was achieved in the human embryonic kidney cell line, HEK293T, according to the published procedure of Lewis *et al.*⁵⁴

Western blot analysis. Denatured total protein from recombinant expressions were loaded onto 4–10% PAGE gels, separated (170 V), then rectilinearly transferred to Trans-Blot® Transfer Medium pure nitrocellulose (BIORAD; 0.45 μ m; 90 V). Immunodetection of hDDAH-1 protein was achieved by probing blots with Goat polyclonal anti-DDAH-1 primary antibody (Abcam®, UK) (1 : 3000 dilution) followed by ImmunoPure® Rabbit anti-Goat IgG used as the secondary antibody (H + L; peroxidase conjugated; Rockford, IL, USA) (1 : 4000 dilution). Immunoreactivity was detected using the BM Chemiluminescence Blotting Substrate (Roche Diagnostics GmbH, Mannheim Germany) and recorded digitally using the FUJIFILM LAS-400 image reader (version 2.0; FUJIFILM Life Science Corporation; Tokyo, Japan) (Fig. 5).

Lysate and pellet fractions of HEK293T cells transfected with pEF-IRES-DDAH-1 (see DDAH-1 cloning and expression) demonstrated immunoreactivity when probed with anti-DDAH-1 primary antibody in contrast to untransfected

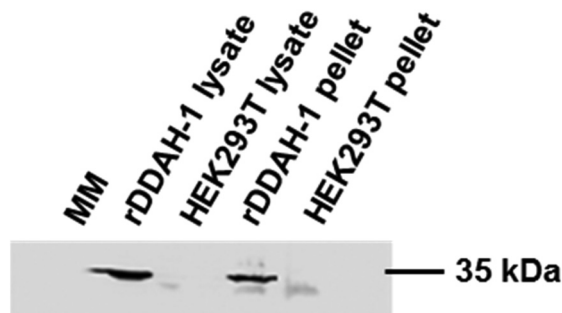


Fig. 5 Immunoblot of human DDAH-1 expression. HEK293T cell lysate (50 μ g) and pellet (50 μ g) were resolved by SDS-PAGE, blotted to nitrocellulose, and probed with anti-DDAH-1 antibody. Molecular weight markers (MM; lane 1), recombinant DDAH-1 lysate (lane 2), untransfected HEK293T control cell lysate (lane 3), recombinant DDAH-1 pellet (lane 4), untransfected HEK293T control cell pellet (lane 5). The immuno-reactive bands occur at 35 kDa.

HEK293T cell lysate and pellet fractions. ColorBurst™ (8–220 kDa; Sigma-Aldrich, Australia) was used as the molecular weight marker (MM).

Measurement of L-citrulline formation by hDDAH-1. L-Citrulline formation was determined in glass tubes at 37 °C in a total incubation volume of 0.1 mL. Incubation mixtures contained HEK293T cell lysate expressing recombinant hDDAH-1 (0.5 mg mL⁻¹), phosphate buffer (0.1 M, pH 7.4) and ADMA (0, 10, 20, 35, 50, 75, 100, 150, 250, 375 and 500 μ M). Deuterated L-citrulline (d6-L-citrulline, 5 mg L⁻¹) was used as the internal standard to correct for random and systemic errors during sample preparation, chromatography and detection. Following a 5 min pre-incubation step (37 °C), reactions were initiated by the addition of substrate (ADMA). Incubations were terminated after 60 min by the addition of 200 μ L of ice-cold acetic acid 4% in methanol. Reaction mixtures were vortex mixed, cooled on ice for 10 minutes, then centrifuged (6000g for 10 min at 10 °C). An aliquot of the supernatant fraction (150 μ L) was diluted into 350 μ L of mobile phase (3 : 10 dilution) and an aliquot of 5 μ L was injected onto the UPLC-MS and monitored according to the method described by Van Dyk *et al.* (2015).⁵⁵ L-Citrulline and ADMA were separated from the matrix in a WATERS ACQUITY T3 HSS C18 analytical column using a Waters ACQUITY Ultra Performance LC™ (UPLC) system. The analyte was separated by gradient elution at a flow rate of 0.2 mL min⁻¹ in a mobile phase comprising 10 mM ammonium formate pH 3.0 in 0.5% methanol (mobile phase A) and 10 mM ammonium formate pH 3.0 in 90% methanol (mobile phase B) with gradient elution at 0.2 ml min⁻¹ over 5 minutes. A WATERS QTOF premier mass spectrometer was used to quantify L-citrulline formation in ESI+ V mode detecting the citrulline fragment with a $m/z = 159.1$. Unknown concentrations of L-citrulline were determined by comparison of the peak area to a calibration curve constructed in the concentration range 0.5 to 25 μ M.

The linearity of L-citrulline formation over time (0–120 min) and over protein concentration (0–1 mg mL⁻¹) was confirmed

in preliminary experiments (data not shown). A protein concentration of 0.5 mg mL^{-1} and incubation time of 60 min was used in all experiments and ensured initial rate conditions with substrate utilization $<20\%$.

Calculation of ADMA kinetic parameters. The rates of L-citrulline formation *versus* substrate concentration ($0\text{--}500 \mu\text{M}$) were model fitted using the nonlinear curve fitting program EnzFitter (version 2.0.18.0: Biosoft, Cambridge, UK). Kinetic constants (K_m , V_{max}) for L-citrulline formation were derived from fitting the Michaelis–Menten equation to experimental data. Goodness of fit was assessed from the F statistic, 95% confidence intervals, r^2 value, and standard error of the parameter fit. Kinetic data are given as the mean of four separate experiments and derived K_m and V_{max} values of $103 \mu\text{M}$ and $258 \text{ pmol min}^{-1} \text{ mg}^{-1}$, respectively (Fig. 6).

Analysis of DDAH inhibition. All compounds synthesized here along with the known DDAH inhibitor L-257 were assessed for their ability to inhibit hDDAH-1 by detecting L-citrulline formation.

Inhibition experiments separately comprised each novel compound and L-257 ($0\text{--}1 \text{ mM}$), HEK293T cell lysate expressing recombinant hDDAH-1 (0.5 mg mL^{-1}), phosphate buffer (0.1 M , pH 7.4) and ADMA ($100 \mu\text{M}$) as the substrate. Following

a 5 min pre-incubation step ($37 \text{ }^\circ\text{C}$), reactions were initiated by the addition of ADMA. Deuterated L-citrulline ($\text{d}_6\text{-L-cit}$, 5 mg L^{-1}) was used as the internal standard. Reactions were terminated and prepared for analysis (see Measurement of citrulline formation by hDDAH-1). Each potential inhibitor was used at five concentrations ($0, 0.1, 1, 10, 100, 1000 \mu\text{M}$ or $0, 0.1, 1, 10, 100, 500 \mu\text{M}$ in the case of 1,2,3-triazoles) for screening studies and five concentrations in the range $0\text{--}75 \mu\text{M}$ in kinetic studies. DMSO in a final concentration of 1% was used in the experiments involving the 1,2,3-triazole compounds in order to permit solubilization.

Data points referring to inhibition screening are the mean of duplicate measurements and kinetic data are represented as Eadie–Hofstee plots. The concentrations of compounds producing 50% of enzyme inhibition (IC_{50}) were calculated using GraphPad Prism 5.0 and these values were derived only for compounds with significant inhibition at 1 mM . Inhibition constants (K_i) were determined by fitting data to the equations for competitive, non-competitive, uncompetitive, and the mixed model of inhibition using Enzfitter. Goodness of fit was assessed from the F statistic, 95% confidence intervals, r^2 value, and standard error of the parameter fit.

In silico analyses

Protein and inhibitor preparation. The structure of hDDAH-1 pdb entry 2JAJ⁵⁷ was used for all studies. The GROMOS force field treats aliphatic hydrogen atoms as united atoms together with the carbon atom to which they are attached. The coordinates of polar hydrogen atoms (bound to nitrogen, oxygen, or sulfur atoms) and aromatic hydrogen atoms were generated based on ideal geometries. In the chain A of pdb 2JAJ, the first 7 N-terminal residues were not resolved in addition to residues 32, 33, 282–284. The coordinates for the missing residues 1–7 and 32, 33 were built using the ModLoop program.⁵⁸ The missing C-terminal residues (282–284) were not included in the model as they are distal to the active-site. The charges of the ionizable groups were chosen to correspond to a pH of 7, resulting into charge of -8 for the system of hDDAH-1, 8 Na^+ ions were added to get a system with net charge of zero. In the presence of L-257 (or **10a**) 7 Na^+ were added to neutralize the system to compensate +1 charge of each ligand. Histidine residues were assigned the appropriate tautomeric configuration based on the local environment of these residues. The protein was placed at the center of a periodic cubic box, which was filled with ~ 9987 SPC water molecules. For the simulations in the presence of L-257 (or **10a**), the initial configurations were obtained by overlaying with X-ray crystal structure of L-257 co-crystallized with DDAH-1.

Molecular dynamics simulations. All molecular dynamics (MD) simulations were performed under periodic conditions using the GROMACS package v. 4.5.4⁵⁹ in conjunction with the GROMOS 53A6 force field.⁶⁰ The initial structure of hDDAH-1 pdb entry 2JAJ⁵⁹ was used for all studies. The topologies of the ligands (L-257 and **10a**) were generated using the ‘Automated Topology Builder’ (ATB, <http://compbio.biosci.uq.edu.au/atb/>)

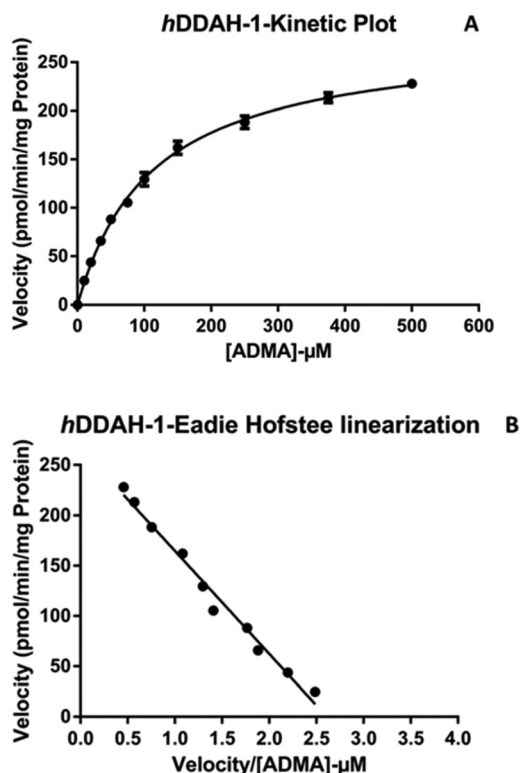


Fig. 6 (A) Rate of reaction (pmol per min per mg protein) *versus* [ADMA] plot of L-citrulline formation by hDDAH-1. (B) Eadie–Hofstee plot for L-citrulline formation induced by hDDAH-1 at different ADMA concentrations. Units of Velocity/[ADMA] are pmol citrulline per μmol per min per mg. Points are experimentally determined values, whereas lines are from model-fitting.

).⁶¹ All systems were energy-minimized using the steepest descent method. Equilibration was then conducted in two phases, during which position restraints were placed on all heavy protein atoms. The first phase applied an NVT ensemble for 250 ps, using the Berendsen weak coupling method⁶² to maintain the temperature of the system at 298 K. The protein and solvent (including ions) were coupled separately. The second phase of equilibration applied an NPT ensemble for 250 ps, using Parrinello–Rahman barostat⁶³ to maintain the pressure at 1 atm. Production MD was then conducted in the absence of any restraints, using the same NPT ensemble. The lengths of all bonds were constrained to ideal values using the P-LINCS algorithm,⁶⁴ with an integration time step of 2 fs. The neighbour list was cut off at 1.4 nm and updated every 5 time steps. All short-range non-bonded interactions were cut off at 1.4 nm, with dispersion correction applied to energy and pressure terms to account for the truncation of van der Waals interactions. Long-range electrostatic interactions were calculated with the smooth particle mesh Ewald method^{65,66} using cubic-spline interpolation and a Fourier grid spacing of approximately 0.16 nm. All analyses were conducted using programs in the GROMACS package. Visualization was done using VMD program.⁶⁷

Acknowledgements

The authors thank eResearch SA for computational time and data storage facility. PCN acknowledges Flinders University for Research Fellowship. The authors would also like to thank Prof. John O. Miners for his helpful suggestions and the opportunity to use the facilities at the Department of Clinical Pharmacology at Flinders University, Dr Andrew Rowland for his help in the development of the hDDAH-1 activity assay and Rhys Murphy for his help in conducting the polarimetry experiments. We thank Prof. James Leiper (MRC Clinical Sciences Centre, London, UK) for a sample of L-257.

We thank also the EPSRC National Mass Spectrometry Service Centre (Swansea, UK), for performing HRMS analyses.

References

- P. Vallance and J. Leiper, *Nat. Rev. Drug Discovery*, 2002, **1**, 939–950.
- M. Colasanti and H. Suzuki, *Trends Pharmacol. Sci.*, 2000, **21**, 249–252.
- S. Moncada, *Ann. N. Y. Acad. Sci.*, 1997, **811**, 60–69.
- C. Napoli and L. J. Ignarro, *Nitric Oxide*, 2001, **5**, 88–97.
- C. Bogdan, *Nat. Immunol.*, 2001, **2**, 907–916.
- M. Rand, *Clin. Exp. Pharmacol. Physiol.*, 1992, **19**, 147–169.
- D. E. Barañano and S. H. Snyder, *Proc. Natl. Acad. Sci. U. S. A.*, 2001, **98**, 10996–11002.
- P. Ferroni, S. Basili, V. Paoletti and G. Davì, *Nutr. Metab. Cardiovasc. Discovery*, 2006, **16**, 222–233.
- V. Hampl and J. Herget, *Physiol. Rev.*, 2000, **80**, 1337–1372.
- C. Baylis, *AJP Ren. Physiol.*, 2007, **294**, F1–F9.
- A. L. Burnett, *J. Clin. Hypertens.*, 2006, **8**, 53–62.
- I. A. Buhimschi, G. R. Saade, K. Chwalisz and R. E. Garfield, *Hum. Reprod. Update*, 1998, **4**, 25–42.
- H. Li and U. Förstermann, *J. Pathol.*, 2000, **190**, 244–254.
- M. A. Titheradge, *Biochim. Biophys. Acta*, 1999, **1411**, 437–455.
- L. Neeb and U. Reuteur, *CNS Neurol. Disord.: Drug Targets*, 2007, **6**, 258–264.
- Y.-C. Hsu, L.-F. Wang and Y. W. Chien, *Free Radical Biol. Med.*, 2007, **42**, 599–607.
- Z.-Y. Wang and R. H. Akanson, *Br. J. Pharmacol.*, 1995, **116**, 2447–2450.
- J. N. Sharma, A. Al-Omran and S. S. Parvathy, *Inflammopharmacology*, 2007, **15**, 252–259.
- D. Fukumura, S. Kashiwagi and R. Jain, *Nat. Rev. Cancer*, 2006, **6**, 521–534.
- P. Pacher, J. S. Beckman and L. Liaudet, *Physiol. Rev.*, 2007, **87**, 315–424.
- D. S. Bredt and S. H. Snyder, *Annu. Rev. Biochem.*, 1994, **63**, 175–195.
- J. Leiper and M. Nandi, *Nat. Rev. Drug Discovery*, 2011, **10**, 277–291.
- O. W. Griffith and D. J. Stuehr, *Annu. Rev. Physiol.*, 1995, **57**, 707–734.
- D. J. Stuehr, *Annu. Rev. Pharmacol. Toxicol.*, 1997, **37**, 339–359.
- S. Anthony, J. Leiper and P. Vallance, *Vasc. Med.*, 2005, **10**, 3–9.
- E. Schwedhelm and R. Böger, *Nat. Rev. Nephrol.*, 2011, **7**, 275–285.
- J. Leiper, J. Santa Maria, A. Chubb, R. J. MacAllister, I. Charles, Gs. Whitley and P. Vallance, *Biochem. J.*, 1999, **343**, 209–214.
- M. Knipp, J. M. Charnock, C. D. Garner and M. Vasak, *J. Biol. Chem.*, 2001, **276**, 40449–40456.
- B. Cillero-Pastor, J. Mateos, C. Fernández-López, N. Oreiro, C. Ruiz-Romero and F. J. Blanco, *Arthritis Rheum.*, 2012, **64**, 204–212.
- K. S. Altmann, A. Havemeyer, E. Beitz and B. Clement, *ChemBioChem*, 2012, **13**, 2599–2604.
- T. Linsky and W. Fast, *J. Biomol. Screen.*, 2011, **16**, 1089–1097.
- J. Kotthaus, D. Schade, N. Muschick, E. Beitz and B. Clement, *Bioorg. Med. Chem.*, 2008, **16**, 10205–10209.
- P. Vallance, H. D. Bush, B. J. Mok, R. Hurtado-Guerrero, H. Gill, S. Rossiter, J. D. Wilden and S. Caddick, *Chem. Commun.*, 2005, 5563–5565.
- S. Rossiter, C. L. Smith, M. Malaki, M. Nandi, H. Gill, J. M. Leiper, P. Vallance and D. L. Selwood, *J. Med. Chem.*, 2005, **48**, 4670–4678.
- Y. Wang, S. Hu, A. J. Gabisi, J. Er, A. Pope, G. Burstein, C. Schardon, A. Cardounel, S. Ekmekcioglu and W. Fast, *ChemMedChem*, 2014, **9**, 792–797.
- J. Kotthaus, D. Schade, J. Kotthaus and B. Clement, *J. Enzyme Inhib. Med. Chem.*, 2012, **27**, 24–28.

- 37 K. Hwa-Ok, M. Felix and O. Cyprian, *Synlett*, 1999, 193–194.
- 38 C. Ballatore, D. M. Huryn and A. B. Smith, *ChemMedChem*, 2013, **8**, 385–395.
- 39 N. A. Meanwell, *J. Med. Chem.*, 2011, **54**, 2529–2591.
- 40 P. K. Chakravarty, E. M. Naylor, A. Chen, R. S. Chang, T.-B. Chen, K. A. Faust, V. J. Lotti, S. D. Kivlighn and R. A. Gable, *J. Med. Chem.*, 1994, **37**, 4068–4072.
- 41 O. N. Ventura, J. B. Rama, L. Turi and J. J. Dannenberg, *J. Am. Chem. Soc.*, 1993, **115**, 5754–5761.
- 42 G. Han, M. Tamaki and V. J. Hruby, *J. Pept. Res.*, 2001, **58**, 338–341.
- 43 Z. P. Demko and K. B. Sharpless, *Org. Lett.*, 2002, **4**, 2525–2527.
- 44 S. Keil, M. Urmann, P. Bernardelli, M. Glien, W. Wendler, K. Chandross and L. Lee, *US Pat.*, 7709481 (B2), 2010.
- 45 R. J. Herr, *Bioorg. Med. Chem.*, 2002, **10**, 3379–3393.
- 46 C. Hansch and L. Leo, *Exploring QSAR. Fundamentals and Applications in Chemistry and Biology*, American Chemical Society, Washington, DC, 1995.
- 47 T. Naka, K. Kubo, Y. Inada and K. Nishikawa, *Drug Discovery*, 1999, **16**, 95–108.
- 48 G. A. Patani and E. J. LaVoie, *Chem. Rev.*, 1996, **96**, 3147–3176.
- 49 J. E. Moses and A. D. Moorhouse, *Chem. Soc. Rev.*, 2007, **36**, 1249.
- 50 T. W. Linsky and W. Fast, *Bioorg. Med. Chem.*, 2012, **20**, 5550–5558.
- 51 H. J. M. Gijzen, M. A. J. De Cleyn, M. Surkyn and B. M. P. Verbist, *US Pat.*, 20130324529 A1, 2013.
- 52 A. S. Thompson, G. R. Humphrey, A. M. DeMarco, D. J. Mathre and E. J. J. Grabowski, *J. Org. Chem.*, 1993, **58**, 5886–5888.
- 53 D. Zornik, R. M. Meudtner, T. El Malah, C. M. Thiele and S. Hecht, *Chem. – Eur. J.*, 2011, **17**, 1473–1484.
- 54 B. C. Lewis, P. I. Mackenzie and J. O. Miners, *Biochem. Pharmacol.*, 2011, **82**, 2016–2023.
- 55 M. Van Dyk, A. A. A. Mangoni, M. McEvoy, J. R. Attia, M. J. Sorich and A. Rowland, *Clin. Chim. Acta*, 2015, **447**, 59–65.
- 56 P. C. Nair and J. O. Miners, *In Silico Pharmacol.*, 2014, **2**, 4.
- 57 J. Leiper, M. Nandi, B. Torondel, J. Murray-Rust, M. Malaki, B. O'Hara, S. Rossiter, S. Anthony, M. Madhani, D. Selwood, C. Smith, B. Wojciak-Stothard, A. Rudiger, R. Stidwill, N. Q. McDonald and P. Vallance, *Nat. Med.*, 2007, **13**, 198–203.
- 58 A. Fiser and A. Sali, *Bioinformatics*, 2003, **19**, 2500–2501.
- 59 B. Hess, C. Kutzner, D. van der Spoel and E. Lindahl, *J. Chem. Theory Comput.*, 2008, **4**, 435–447.
- 60 C. Oostenbrink, A. Villa, A. E. Mark and W. F. Van Gunsteren, *J. Comput. Chem.*, 2004, **25**, 1656–1676.
- 61 A. K. Malde, L. Zuo, M. Breeze, M. Stroet, D. Poger, P. C. Nair, C. Oostenbrink and A. E. Mark, *J. Chem. Theory Comput.*, 2011, **7**, 4026–4037.
- 62 H. J. C. Berendsen, J. P. M. Postma, W. F. van Gunsteren, A. DiNola and J. R. Haak, *J. Chem. Phys.*, 1984, **81**, 3684–3690.
- 63 M. Parrinello, *J. Appl. Phys.*, 1981, **52**, 7182–7190.
- 64 B. Hess, *J. Chem. Theory Comput.*, 2008, **4**, 116–122.
- 65 T. Darden, D. York and L. Pedersen, *J. Chem. Phys.*, 1993, **98**, 10089–10092.
- 66 U. Essmann, L. Perera, M. L. Berkowitz, T. Darden, H. Lee and L. G. Pedersen, *J. Chem. Phys.*, 1995, **103**, 8577–8593.
- 67 W. Humphrey, A. Dalke and K. Schulten, *J. Mol. Graphics*, 1996, **14**, 33–38.